CDF/ANAL/EXOTIC/CDFR/9299
Version 1.0
May 9, 2008

Search for the Standard Model Higgs Boson Production in Association with $W^{\pm}$ Boson Using Isolated Tracks in $\int \mathcal{L}dt$ = 2.1 fb^{-1}

Adrian Buzatu[9], Jay Dittmann[1], Pedro Fernandez[7], Martin Frank[1], Richard Hughes[2], Shinhong Kim[6], Nils Krumnack[1], Kevin Lannon[2], Tatsuya Masubuchi[6], Yoshikazu Nagai[6], Jason Nielsen[5], Thomas Mullar[8], Thomas Peiffer[8], Jason Slaunwhite[2], Rob Snihur[9], Anyes Taffard[3], Jeannine Wagner-Kuhr[8], Wolfgang Wagner[8], Andreas Warburton[9], Brian Winer[2], Weiming Yao[4]

[1]*Baylor University*
[2]*Ohio State University*
[3]*UC Irvine*
[4]*LBNL*
[5]*UC Santa Cruz*
[6]*University of Tsukuba*
[7]*FNAL*
[8]*Karlsruhe*
[9]*McGill*

Abstract

We present a search for Standard Model Higgs boson production in association with a $W^{\pm}$ boson. This search uses data through period 13, corresponding to an integrated luminosity of $2.1\mathrm{fb}^{-1}$. We select W candidate events recorded by the $\not\!\!E_T$ plus jet trigger that have 2 jets, large $\not\!\!E_T$, and isolated track lepton candidate. Discrimination between the Higgs signal and the large backgrounds in the $W + 2$ jet bin is increased through the use of an artificial neural net. We see no evidence for a Higgs signal, so we set a 95% confidence level upper limit on the WH cross section times the branching ratio of the Higgs to decay to a $b\bar{b}$ pair by fitting the neural network output distribution:

$$\sigma(p\bar{p} \rightarrow W^{\pm}H) \times BR(H \rightarrow b\bar{b})|_{M(H)=120} < 15.7 \times \text{SM}$$

We set limits across a range of Higgs masses. The limts range from $\sigma(p\bar{p} \rightarrow W^{\pm}H) \times BR(H \rightarrow b\bar{b}) < 11.3$ to 126.1 times the standard model for Higgs masses from 110 GeV/c^2 to 150 GeV/c^2

1 Introduction

This note describes the search for $p\bar{p} \rightarrow WH \rightarrow \ell\nu b\bar{b}$ in events that have at least one SECVTX b-tagged jet. The signature for this process is a W-boson, decaying to a high-p_T charged lepton and neutrino, and two jets containing b-quarks (see Figure 1). This signature is primarily sensitive for low Higgs masses where the $H \rightarrow b\bar{b}$ branching fraction is large, as shown in Figure 2. The main backgrounds for this process include $W + 2$ jet production (where the jets contain either tagged heavy flavor or mistagged light flavor), $t\bar{t}$ production, and QCD multijet production, where one jet fakes a lepton. These background processes are essentially the same as the backgrounds for the $t\bar{t}$ search in the $W+ \geq 3$ jet bin, although in the case of $t\bar{t}$ the ratio of signal to background is much higher. This search uses data collected up to August 2007, which corresponds to a total integrated luminosity of 2.1fb^{-1}.

The previous WH search [1] was performed with integrated luminosity of 1.9fb^{-1}and set an upper limit on the production cross section as shown in Figure 3. The 1.9fb^{-1}result used data collected with high-p_T lepton triggers. This version of the analysis uses loose lepton identification requirements to identify WH candidate events in data collected with $\not\!\!E_T$ plus jet triggers. We define a single category of loose lepton identification called Isolated Track (ISOTRK). The isolated track category is defined to be exclusive to the tight lepton selection to facilitate combination. After identifying WH candidate events in this new triggger stream we apply the same background estimate and search techniques as the high-p_T lepton triggered version of the analysis. Ultimately, we combine the searches in the two different trigger stream to obtain optimal overall sensitivity.

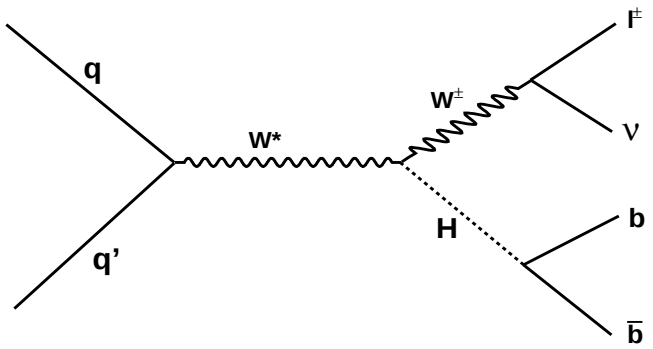

Figure 1: Feynman diagram of WH production.

2 Data/MC samples and Luminosity Calculation

We use data collected in datasets `emetmd, emetmh, emetmi, emetmj`. We select events from these datasets that pass one of the following $\not\!\!E_T$ plus jet triggers:

1. `MET35_&_TWO_JETS`

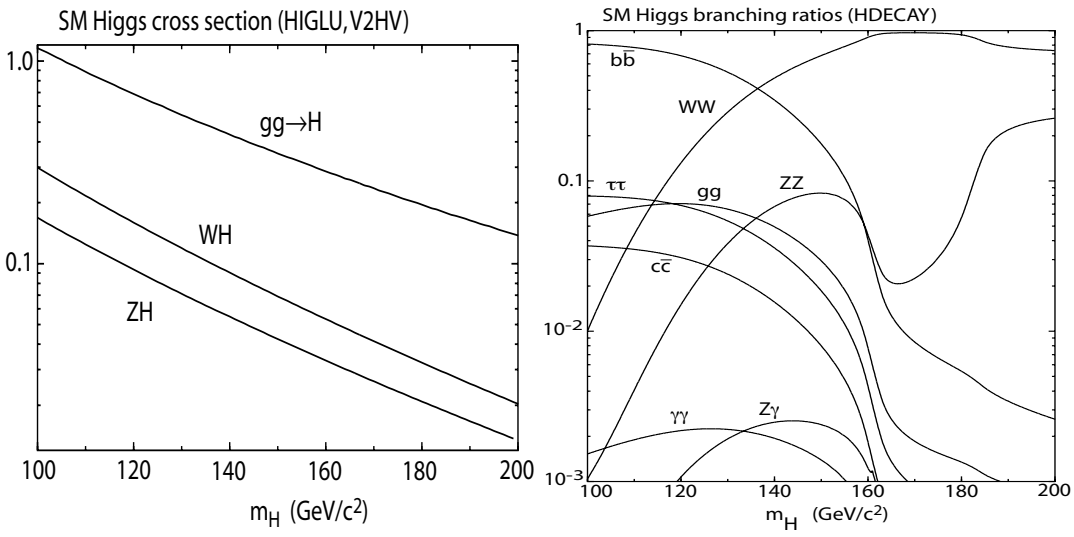

Figure 2: Standard model Higgs boson production cross section at the Tevatron and the branching ratio of Higgs boson.

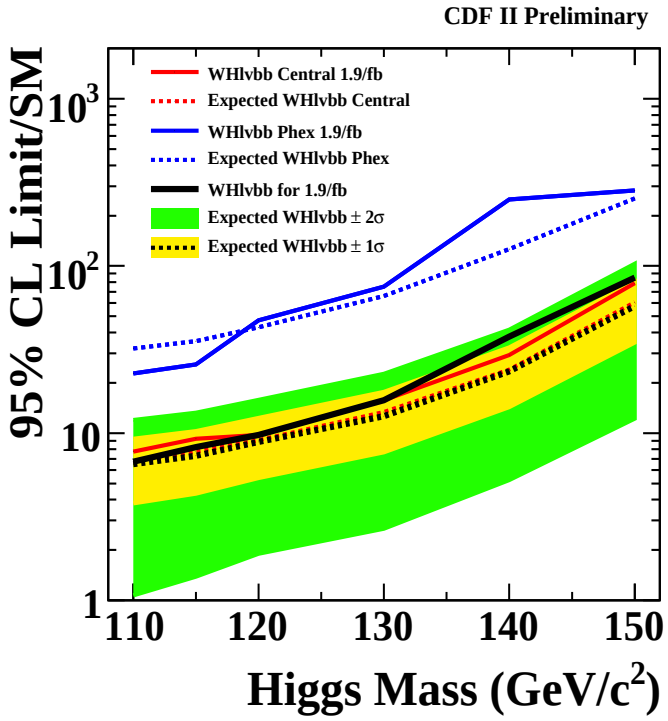

Figure 3: Upper limit on $\sigma(p\bar{p} \rightarrow WH) \times BR(H \rightarrow b\bar{b})$ obtained with 1.9fb^{-1}of high-p_T lepton triggered data.

2. MET35_&_CJET_&_JET
3. MET35_&_CJET_&_JET_LUMI_190
4. MET35_&_CJET_&_JET_DPS

Due to trigger bandwidth considerations at high luminosities we use "luminosity enabled" (LUMI_190) and "dynamically prescaled"(DPS) triggers. Luminosities are calculated using the DQM version 19 silicon good run list (bits [1,1,4,1]), taking into account the changing prescales of the luminosity enabled and DPS triggers [2]. The corresponding total integrated luminosity is 2.10 fb^{-1}.

Our Higgs signal model comes from the official Higgs Discovery Group Higgs Monte Carlo (MC) samples generated with PYTHIA using the standard MC procedure outlined in CDF software version 6.1.4. These Higgs samples were generated for a range of Higgs masses (M_h = 110, 115, 120, 130, 140 and 150 GeV). Our background models are composed of a number of components. The W and Z plus light flavor and heavy flavor jet processes are modeled using ALPGEN version 2.10 showered with PYTHIA. Likewise, the single-top contribution is modeled using parton-level events generated by MadEvent and showered through PYTHIA. The rest of the background processes, including the $t\bar{t}$, WW, WZ, and ZZ processes were generated with PYTHIA. For backgrounds involving a top quark, the top mass was set to 175 GeV/c^2.

3 Event Selection

We select events that contain an isolated track with p_T > 20 GeV, offline corrected $\not\!\!E_T$ > 20 GeV, and exactly two jets with cone size 0.4 and corrected E_T > 20 GeV. We also apply cuts so that the jet part of the $\not\!\!E_T$ plus jets trigger is fully efficient. We discuss the isolated track selection and trigger efficiency cuts in the sub-sections that follow.

3.1 Isolated track selection

We select high quality, high-p_T isolated tracks using the selection criteria outline in Table 1. Our selection is based on the top lepton+track cross section measurement [3].

We define the proximity of our tracks to other activity in the event using track isolation. Track isolation uses only track information and no calorimeter information. It is defined as,

$$\text{TrkIsol} = \frac{p_T(candiate)}{p_T(candiate) + \sum p_T(trk)} \quad (1)$$

where $\sum p_T(trk)$ is the sum of the p_T of tracks that meet the following requirements:

- $p_T > 0.5$ GeV
- ΔR(trk, candidate) < 0.4

Variable	Cut
p_T	> 20 GeV
$\|z_0\|$	< 60 cm
$\|d_0\|corr$	< 0.2
$\|d_0\|corr$ (w/SI)	< 0.02
track isolation	> 0.9
Axial COT hits	≥ 24
Stereo Hits	≥ 20
χ^2 probability (data only)	$> 10^{-8}$
Num Si Hits (data only, only if num expect ≥ 3)	≥ 3

Table 1: Isolated track selection cuts

- ΔZ(trk, candidate) < 5 cm
- Number of COT axial hits > 20
- Number of COT stereo hits > 10

Using this definition, a track with no surrounding activity has a isolation of 1.0. We require track isolation > 0.9, or 90% of the local track p_T .

We use a variety of vetos that ensure that isolated tracks events are from W events and that they do not overlap other lepton identifications.

- **Tight Jet Veto**: We veto isolated tracks with an angular separation $\Delta R < 0.4$ from any tight jet in the event.
- **Two Track Veto**: We count the number of isolated tracks in the event before applying the tight jet veto. If there are two or more isolated tracks, we veto the event.
- **Tight Lepton Veto**: We check to see if any any CEM, CMUP, or CMX leptons in the event. If any tight isolated leptons are found we do not allow the event to pass isotrk selection.

3.2 Jets Trigger Requirements

We define a tight jet to have cone size 0.4, $E_T > 20$ GeV after level 5 jet corrections (using `jetCorr12`), and $|\eta_{Detector}| < 2.0$. This selection is identical to the tight lepton analysis.

The $\not\!\!E_T$ plus jets trigger has been used extensively in the $VH \rightarrow \not\!\!E_T + b\bar{b}$ Higgs search [4] [5], and also in the Single Top search, [6]. Those studies have shown that the trigger's jet requirements are fully efficient after the following cuts:

- Two Tight Jets with $E_T > 25$ GeV

- $\Delta R < 1.0$
- One central jet with $|\eta| < 1.0$

We apply these additional jet cuts after identifying the tight jets in the event. For jet bins ≥ 3, we require that the two lead jets in the event satisfy these requirements.

3.3 Missing Et Trigger Parameterization

We parameterize the $\not\!\!E_T$ trigger turn-on as a function of vertex $\not\!\!E_T$ as shown in figure 4. We choose vertex $\not\!\!E_T$, which is corrected for the primary vertex position but not muons or jet energy scale, because this quantity is closely related to trigger-level $\not\!\!E_T$. We measure the $\not\!\!E_T$ plus jets trigger turn-on following the proceedure outlined in [6] using events recorded with the CMUP trigger. We define the the trigger efficiency as the number of CMUP events passing the trigger jet requirements that fired the $\not\!\!E_T$ plus jets trigger.

We account for the effects of the trigger turn-on by weighting each event that passes our other selection criteria by its probablity to pass the $\not\!\!E_T$ trigger.

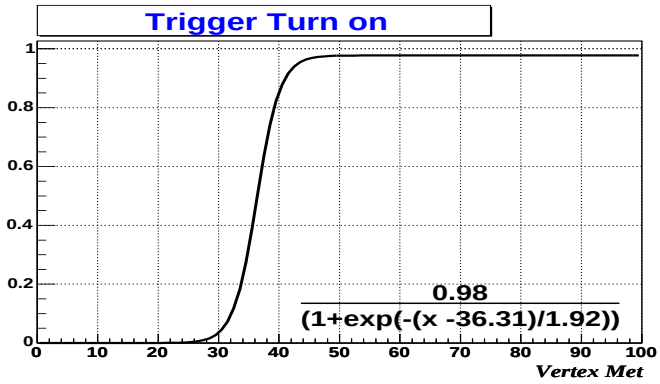

Figure 4: $\not\!\!E_T$ plus jets trigger turn-on curve parameterized as a function of vertex $\not\!\!E_T$.

3.4 Other Event Selection Cuts

After identifying events with an isolated track and passing the $\not\!\!E_T$ trigger turn-on requirements we apply the same selection criteria as the lepton-triggered analysis, including a cut on 20 GeV of $\not\!\!E_T$ corrected for muons and jet energy scale, a dilepton veto, a cut on the separation between the isolated track z-vetex and the jet z-vertex, a Z boson veto, and a cosmic ray veto.

3.5 B-tagging

We use two categories of b-tagged events: double-tagged (ST+ST) and single-tagged (EQ1TAG). We will extend our b-tagging categories to match the categories of the high-pt lepton triggered analysis in a future update.

4 Background

We use the same methodology of background estimation as the lepton-triggered analysis, which is closely related to the background estimate used in the $t\bar{t}$ cross section measurement [7]. The estimate is generally called "Method II". The version of the background estimate used in this analysis is documented in detail in the CDF note "Method II For You" [8].

In the W+jets sample, the following background sources are considered:

Non-W QCD: A W signature is generated when one jet fakes a high p_T lepton and $\not\!\!E_T$ is generated through jet energy mismeasurement.

W + Mistags: This background occurs when one or more light flavor jets produced in association with a W boson are mistakenly identified as a heavy flavor jet by the b-tagging algorithms. Mistags are generated because of the finite resolution of the tracking, because of material interactions, or because of long-lived light flavor hadrons (Λ and K_s) that produce displaced vertices.

W+ Heavy Flavor: These processes ($W + b\bar{b}$, $W + c\bar{c}$ and $W + c$) involve the production of actual heavy flavor quarks in association with a W boson.

Top Quark Backgrounds: This background comes both from single top quark production and top quark pair production.

Other EWK Backgrounds: Additional small background contributions come from Z + jets production and diboson (WW, WZ, and ZZ) production.

Follwing the same approach as the "Method II for You" code and the single top analysis, we determine the amount of non-w by fitting the $\not\!\!E_T$ distribution of the pretag, one secvtx tag, and double secvtx tagged samples. We estimate the W + Mistag background by applying the mistag matrix to the pretag $W+$ jets data after subtracting the non-W, top, diboson, Z+jets and W+HF contributions. We model the W + Mistag kinematics using $W+$ light flavor Monte Carlo events. The W + Heavy Flavor background is also estimated from the pretag data using ALPGEN + PYTHIA MC to set the relative normalization of light to heavy flavor events as well as the b-tagging efficiency for W + Heavy Flavor events (see below). The top quark and other EWK backgrounds are normalized directly to their theoretical cross sections, calculated at next-to-leading order. We expand upon the details of be background in the sections that follow. Additional information can be found in "Method II For You" [8].

4.1 NonW (QCD fake) background

We estimate the non-W fraction in the pretag and tag samples by fitting the data $\not\!\!E_T$ distribution with a non-W template and a MC signal template. The non-W template is obtained from non-isolated (iso > 0.1) loose muon events in the $\not\!\!E_T$ plus jets trigger. The MC signal tempalte contains events from Z+jet, W+LF, top, and EWK backgrounds. We use the same uncertainty as "Method II For You" [8], which was determined by performing fits with a variety of binings and fit ranges. The relative uncertainty on the non-W normalization is 40%. Figures 5 through 7 show the results fitting the $\not\!\!E_T$ distribution in the pretag and tag regions. The fits in the double tagged region suffers from low statistics. The uncertainty of 40% accomodates the low statistics

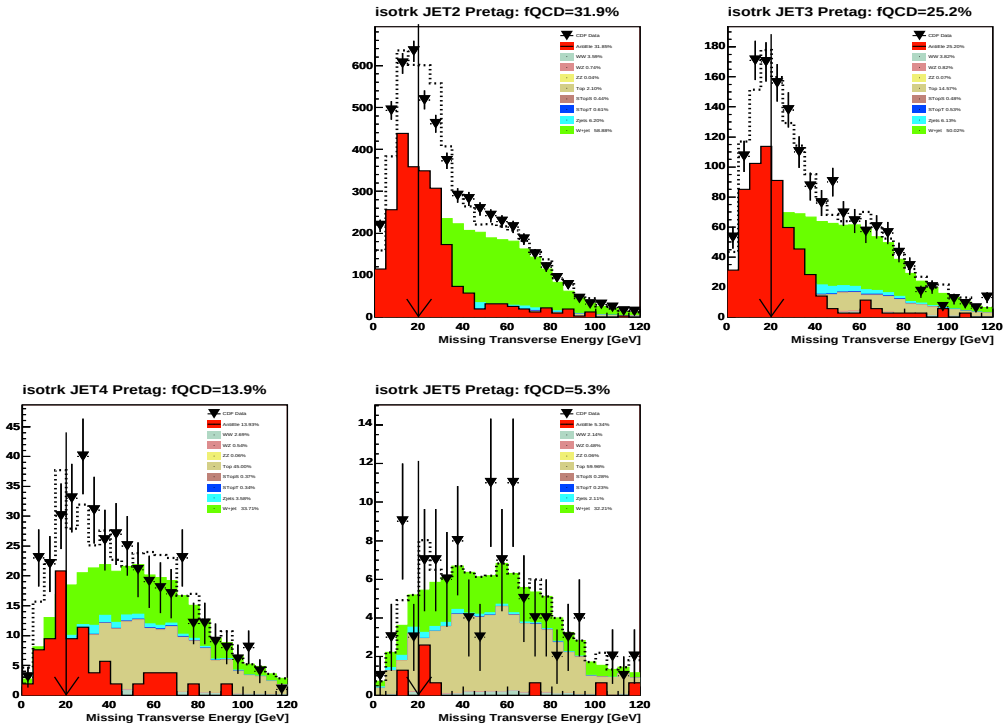

Figure 5: QCD fraction estimate for pretag events

4.2 W + Heavy Flavor

The $Wb\bar{b}$ and $Wc\bar{c}$ states are major sources of background events with real b-tags in the W+jets channel. They are estimated primarily from the Monte Carlo, but their overall rates are normalized to data. The contribution from true heavy flavor production in W+jet events is determined from measurements of the heavy flavor event fraction in $W+$jet events and the tagging efficiency for those events.

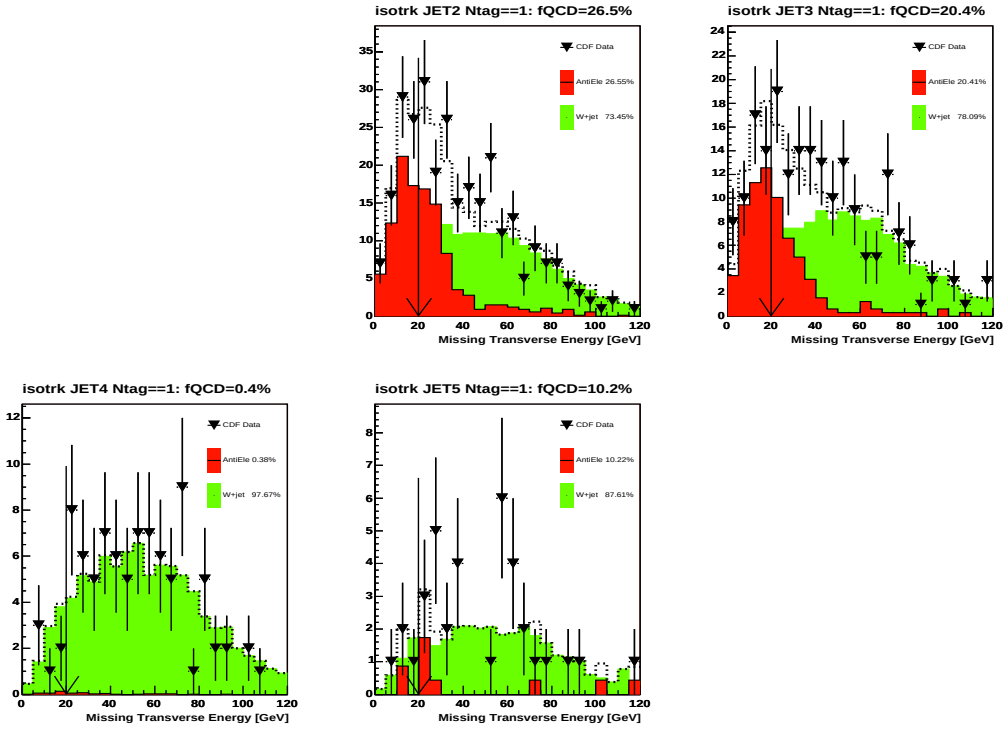

Figure 6: QCD fraction estimate for one SECVTX tag events

These heavy flavor fractions and a scaling factor for these fractions (k-factor) have been studied extensively elsewhere [7, 13] using ALPGEN v2 + PYTHIA Monte Carlo. Heavy flavor fractions measured in ALPGEN have been calibrated using a sample of $W + 1$ jet events, and it is found that a k-factor of 1.4 ± 0.4 is necessary to make the heavy flavor production in Monte Carlo match the production in data. We have calculated the tagging rates and heavy flavor fraction for events passing our selection using the "Method II For you" framework [8]. Tables 2 and 3 summarize our results. We estimate the number of W + heavy flavor events in our tag sample according to

$$N_{W+HF} = f_{HF} \cdot \epsilon_{\text{tag}} \cdot [N_{\text{pretag}} \cdot (1 - f_{\text{non}-W}) - N_{\text{EWK}}] \,, \tag{2}$$

where f_{HF} is heavy fraction, ϵ_{tag} is tagging efficiency and N_{EWK} is the expected number of $t\bar{t}$, single top, $Z+$ jets, and diboson events.

4.3 Mistag

The rate of W + mistag, or falsely tagged, jets is derived from a sample of events collected with a jet-based trigger with no heavy flavor requirement. The mistag rate is obtained using negative tags, which are tags that appear to come from behind the primary vertex. The mistag rate obtained from negative tags is parameterized in bins of η, jet E_T, track multiplicity

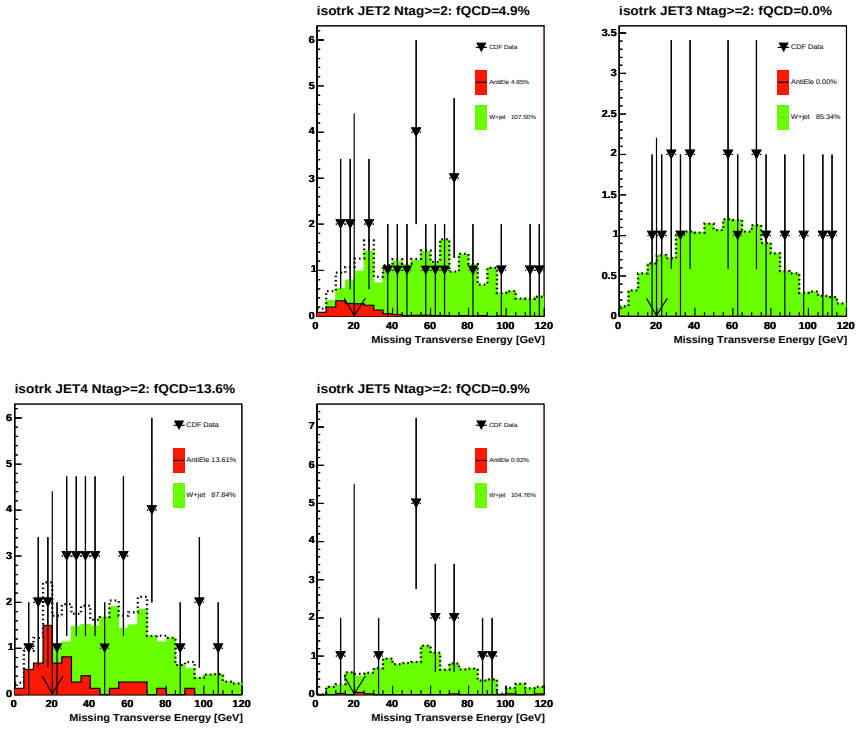

Figure 7: QCD fraction estimate for two SECVTX tag events

Flavor Content	2 Jets	3 Jets	4 Jets	5 Jets
HF1b	2.21	3.58	4.66	5.51
HF2b	1.33	2.64	4.21	6.07
HF1c	11.00	13.92	15.22	15.62
HF2c	2.11	4.67	7.73	10.84

Table 2: Heavy flavor fractions measured in the isotrk sample from ALPGEN v2 W+jets MC.

within a jet, $\sum E_T$ of the event, number of z vertices, and the z vertex position [14]. The mistag rate derived from negative tags is corrected for the effects of heavy flavor in the jet sample, long-lived light flavor vertices, and vertices caused by material interactions in the silicon detector. This correction is parameterized as a function of E_T to reduce its systematic uncertainty [15].

The total mistag rate is estimated from the pretag data. For each pretag event, the mistag probability for each jet is calculated as described above. These probabilities are then used to calculate the probability for that event to be singly or doubly tagged. The sum of the single-tag or double-tag probabilities for all pretag events provides the total mistag estimate. This estimate is then corrected for the fraction of the pretag sample estimated to come from other

Tagg Eff	2 Jets	3 Jets	4 Jets	5 Jets
1 Secvtx Tag Eff				
Eff1b	23.69	25.08	25.71	27.57
Eff2b	30.33	30.41	30.26	30.22
Eff1c	7.15	7.84	8.88	10.16
Eff2c	9.57	10.53	11.40	12.31
2 Secvtx Tag Eff				
Eff1b	0.31	0.80	1.37	1.84
Eff2b	9.04	9.79	10.29	10.85
Eff1c	0.04	0.12	0.25	0.39
Eff2c	0.40	0.58	0.86	0.97

Table 3: Heavy flavor tagging efficiency calculated from ALPGEN v2 W+jets MC for single and double b-tagging categories. The tagging efficiency is expressed relative to the pretag

processes (non-W, top, $Z+$ jets, or dibosons).

The uncertainty on the mistag estimate includes the statistical errors from the matrix itself, accounting for correlations between jets which fall in the same bin of the mistag matrices, and an additional 5.9% error from all systematic uncertainties [14]. Although the mistag matrix was derived using the 1.12fb^{-1}sample, it has been shown that it is acceptable to apply this at least through period 13 data as long as the systematic uncertainties are increased by 1.8% to cover possible discrepancies.

4.4 MC derived background

The normalization of the diboson, $t\bar{t}$ and single top backgrounds are based on the theoretical cross sections (listed in Table 4), the measured luminosity and the acceptance and b-tagging efficiency derived from MC. The MC acceptance is corrected for lepton identification, trigger efficiencies and z vertex cut. The tagging efficiency is always scaled by the MC/data scale factor of 0.95$\pm$ 0.05 for SECVTX tags. The expected number of events is obtained by the equation

$$N = \int \mathcal{L}dt \times \epsilon_{pretag} \times \epsilon_{tag} \times \sigma, \tag{3}$$

where ϵ_{pretag} is the total pretag detection efficiency corrected by all of the scale factors. The tagging efficiency ϵ_{tag} is calculated by summing over the probability to tag each jet in a pretag event. Heavy flavor jets have a tag probability equal to the SECVTX scale factor. Light flavor jets have a probability determined by the mistag matrix. The uncertainties on the normalizations are dervied from measuring the change in acceptance when the tag probabilities are shifted by $\pm$ 1 σ.

Theoretical Cross Sections	
WW	12.4 $\pm$ 0.25 pb
WZ	3.96 $\pm$ 0.06 pb
ZZ	1.58 $\pm$ 0.05 pb
Single Top s-channel	0.88 $\pm$ 0.05 pb
Single Top t-channel	1.98 $\pm$ 0.08 pb
$Z+$ jets	787.4 $\pm$ 50.0 pb
$t\bar{t}$	6.7 $\pm$ 0.08 pb

Table 4: Theoretical cross sections and errors for the electroweak and single top backgrounds, along with the theoretical cross section for $t\bar{t}$ at ($m_t = 175$GeV/c^2).

4.5 Background Summary

We have described the contributions of individual background sources to the final background estimate. The summary table of the background estimates are shown in Tables 5-6 and number of expected events and observed data as a function of jet multiplicity plots are shown in Figure 8 - 9. In general, the number of expected events and the number of observed events are in good agreement.

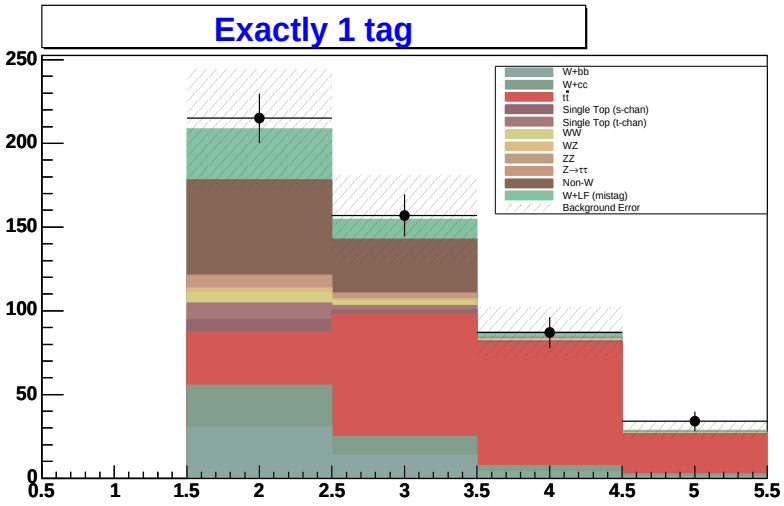

Figure 8: Number of expected one SECVTX tag events for each background in each jet bin, shown with observed number of data events.

Process	2jets	3jets	4jets	5jets
All Pretag Candidates	3708.0 ± 0.0	1150.0 ± 0.0	354.0 ± 0.0	97.0 ± 0.0
Pretag (before MET cut) ww	148.4 ± 9.5	47.4 ± 3.0	10.1 ± 0.7	2.1 ± 0.1
Pretag (before MET cut) wz	31.9 ± 2.0	10.9 ± 0.7	2.2 ± 0.1	0.5 ± 0.0
Pretag (before MET cut) zz	2.5 ± 0.2	1.2 ± 0.1	0.3 ± 0.0	0.1 ± 0.0
Pretag (before MET cut) top	77.8 ± 10.4	178.6 ± 23.9	179.3 ± 24.0	61.8 ± 8.3
Pretag (before MET cut) stops	17.5 ± 1.6	5.9 ± 0.5	1.4 ± 0.1	0.3 ± 0.0
Pretag (before MET cut) stopt	24.8 ± 2.5	6.6 ± 0.7	1.3 ± 0.1	0.2 ± 0.0
Pretag (before MET cut) zlf	376.8 ± 33.2	105.4 ± 9.3	17.9 ± 1.6	2.8 ± 0.2
Total Pretag MC (before MET cut)	679.6 ± 48.9	355.9 ± 31.2	212.5 ± 25.1	67.9 ± 8.5
Pretag QCD	1181.0 ± 472.4	289.8 ± 115.9	49.3 ± 19.7	5.2 ± 2.1
Pretag (after MET cut) ww	130.1 ± 8.4	42.3 ± 2.8	9.1 ± 0.7	1.9 ± 0.2
Pretag (after MET cut) wz	27.1 ± 1.7	9.2 ± 0.6	1.8 ± 0.1	0.4 ± 0.0
Pretag (after MET cut) zz	1.6 ± 0.1	0.8 ± 0.1	0.2 ± 0.0	0.1 ± 0.0
Pretag (after MET cut) top	72.6 ± 9.9	163.5 ± 22.0	164.0 ± 22.1	55.8 ± 7.6
Pretag (after MET cut) stops	15.9 ± 1.5	5.4 ± 0.5	1.2 ± 0.1	0.3 ± 0.0
Pretag (after MET cut) stopt	22.5 ± 2.3	6.0 ± 0.6	1.2 ± 0.1	0.2 ± 0.0
Pretag (after MET cut) zlf	219.2 ± 19.3	69.4 ± 6.1	12.5 ± 1.1	2.0 ± 0.2
Total Pretag MC (after MET cut)	489.0 ± 34.3	296.7 ± 27.1	190.0 ± 22.9	60.7 ± 7.7
Total Pretag HF	324.0 ± 124.4	133.8 ± 48.9	35.2 ± 13.9	10.9 ± 4.2
Total Pretag Corrected	2038.0 ± 473.6	563.5 ± 119.1	114.7 ± 30.2	31.1 ± 8.0
Total LF Pretag Corrected	1713.9 ± 489.7	429.7 ± 128.7	79.5 ± 33.2	20.3 ± 9.0
Tagged ww	6.2 ± 0.7	2.8 ± 0.3	0.8 ± 0.1	0.3 ± 0.0
Tagged wz	2.8 ± 0.2	1.1 ± 0.1	0.2 ± 0.0	0.1 ± 0.0
Tagged zz	0.2 ± 0.0	0.1 ± 0.0	0.0 ± 0.0	0.0 ± 0.0
Tagged top	31.6 ± 4.3	73.1 ± 9.9	73.4 ± 9.9	23.9 ± 3.2
Tagged stops	7.4 ± 0.7	2.4 ± 0.2	0.6 ± 0.1	0.1 ± 0.0
Tagged stopt	9.9 ± 1.1	2.6 ± 0.3	0.5 ± 0.1	0.1 ± 0.0
Tagged zlf	7.4 ± 0.8	3.6 ± 0.4	0.9 ± 0.1	0.2 ± 0.0
Raw Mis-tags(info)	65.6 ± 7.5	32.1 ± 3.7	13.5 ± 1.5	5.9 ± 0.7
Tagged Wbb	30.3 ± 13.5	13.8 ± 6.0	4.1 ± 1.9	1.5 ± 0.7
Tagged Wcc/Wc	25.4 ± 11.5	11.2 ± 4.9	3.4 ± 1.6	1.1 ± 0.5
Tagged Total HF	55.7 ± 23.2	25.1 ± 10.3	7.5 ± 3.2	2.5 ± 1.1
Tagged Total MC	65.5 ± 6.1	85.8 ± 10.4	76.4 ± 10.0	24.6 ± 3.2
Tagged Mistags	30.3 ± 9.3	12.0 ± 3.8	3.0 ± 1.3	1.2 ± 0.6
Tagged Non-W	57.1 ± 22.8	32.0 ± 12.8	0.3 ± 0.5	0.1 ± 0.5
Total Prediction	208.6 ± 34.4	154.9 ± 19.8	87.3 ± 10.6	28.5 ± 3.5
Observed	215.0 ± 0.0	157.0 ± 0.0	87.0 ± 0.0	34.0 ± 0.0

Table 5: Method 2 background estimate for isolated track events with one SECVTX tag.

Process	2jets	3jets	4jets	5jets
All Pretag Candidates	3708.0 ± 0.0	1150.0 ± 0.0	354.0 ± 0.0	97.0 ± 0.0
Pretag (before MET cut) ww	148.4 ± 9.5	47.4 ± 3.0	10.1 ± 0.7	2.1 ± 0.1
Pretag (before MET cut) wz	31.9 ± 2.0	10.9 ± 0.7	2.2 ± 0.1	0.5 ± 0.0
Pretag (before MET cut) zz	2.5 ± 0.2	1.2 ± 0.1	0.3 ± 0.0	0.1 ± 0.0
Pretag (before MET cut) top	77.8 ± 10.4	178.6 ± 23.9	179.3 ± 24.0	61.8 ± 8.3
Pretag (before MET cut) stops	17.5 ± 1.6	5.9 ± 0.5	1.4 ± 0.1	0.3 ± 0.0
Pretag (before MET cut) stopt	24.8 ± 2.5	6.6 ± 0.7	1.3 ± 0.1	0.2 ± 0.0
Pretag (before MET cut) zlf	376.8 ± 33.2	105.4 ± 9.3	17.9 ± 1.6	2.8 ± 0.2
Total Pretag MC (before MET cut)	679.6 ± 48.9	355.9 ± 31.2	212.5 ± 25.1	67.9 ± 8.5
Pretag QCD	1181.0 ± 472.4	289.8 ± 115.9	49.3 ± 19.7	5.2 ± 2.1
Pretag (after MET cut) ww	130.1 ± 8.4	42.3 ± 2.8	9.1 ± 0.7	1.9 ± 0.2
Pretag (after MET cut) wz	27.1 ± 1.7	9.2 ± 0.6	1.8 ± 0.1	0.4 ± 0.0
Pretag (after MET cut) zz	1.6 ± 0.1	0.8 ± 0.1	0.2 ± 0.0	0.1 ± 0.0
Pretag (after MET cut) top	72.6 ± 9.9	163.5 ± 22.0	164.0 ± 22.1	55.8 ± 7.6
Pretag (after MET cut) stops	15.9 ± 1.5	5.4 ± 0.5	1.2 ± 0.1	0.3 ± 0.0
Pretag (after MET cut) stopt	22.5 ± 2.3	6.0 ± 0.6	1.2 ± 0.1	0.2 ± 0.0
Pretag (after MET cut) zlf	219.2 ± 19.3	69.4 ± 6.1	12.5 ± 1.1	2.0 ± 0.2
Total Pretag MC (after MET cut)	489.0 ± 34.3	296.7 ± 27.1	190.0 ± 22.9	60.7 ± 7.7
Total Pretag HF	324.0 ± 124.4	133.8 ± 48.9	35.2 ± 13.9	10.9 ± 4.2
Total Pretag Corrected	2038.0 ± 473.6	563.5 ± 119.1	114.7 ± 30.2	31.1 ± 8.0
Total LF Pretag Corrected	1713.9 ± 489.7	429.7 ± 128.7	79.5 ± 33.2	20.3 ± 9.0
Tagged ww	0.0 ± 0.0	0.1 ± 0.0	0.1 ± 0.0	0.0 ± 0.0
Tagged wz	0.6 ± 0.1	0.2 ± 0.0	0.0 ± 0.0	0.0 ± 0.0
Tagged zz	0.0 ± 0.0	0.0 ± 0.0	0.0 ± 0.0	0.0 ± 0.0
Tagged top	6.8 ± 1.1	20.3 ± 3.3	28.6 ± 4.6	10.3 ± 1.6
Tagged stops	2.4 ± 0.3	0.8 ± 0.1	0.2 ± 0.0	0.0 ± 0.0
Tagged stopt	0.5 ± 0.1	0.5 ± 0.1	0.2 ± 0.0	0.0 ± 0.0
Tagged zlf	0.4 ± 0.1	0.3 ± 0.0	0.1 ± 0.0	0.0 ± 0.0
Raw Mis-tags(info)	0.4 ± 0.1	0.4 ± 0.1	0.2 ± 0.1	0.2 ± 0.0
Tagged Wbb	4.7 ± 2.1	2.3 ± 1.0	0.8 ± 0.4	0.3 ± 0.1
Tagged Wcc/Wc	0.4 ± 0.2	0.4 ± 0.2	0.1 ± 0.1	0.1 ± 0.0
Tagged Total HF	5.2 ± 2.3	2.7 ± 1.2	1.0 ± 0.4	0.4 ± 0.2
Tagged Total MC	10.8 ± 1.4	22.3 ± 3.4	29.2 ± 4.6	10.4 ± 1.7
Tagged Mistags	0.2 ± 0.1	0.1 ± 0.1	0.1 ± 0.0	0.0 ± 0.0
Tagged Non-W	0.9 ± 0.4	0.0 ± 0.5	3.5 ± 2.8	1.6 ± 1.3
Total Prediction	17.1 ± 2.7	25.1 ± 3.6	33.7 ± 5.4	12.5 ± 2.1
Observed	19.0 ± 0.0	19.0 ± 0.0	26.0 ± 0.0	12.0 ± 0.0

Table 6: Method 2 background estimate for isolated traack events with ≥ 2 SECVTX tags.

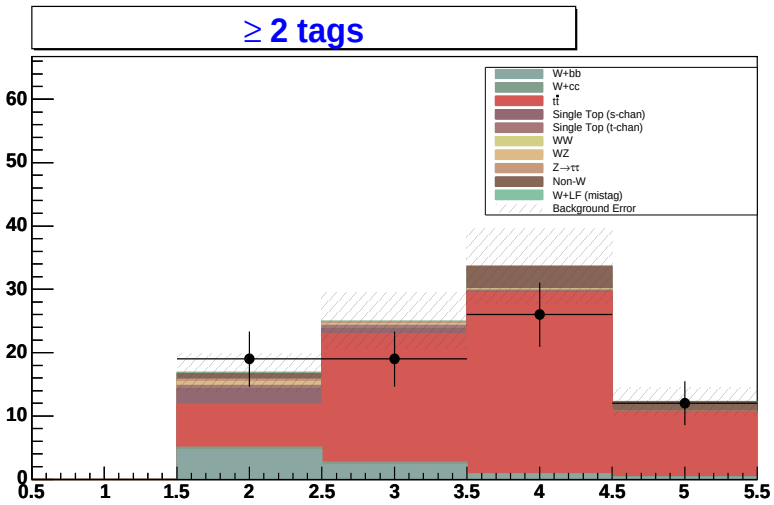

Figure 9: Number of expected one SECVTX tag events for each background in each jet bin, shown with observed number of data events.

5 Higgs Signal Acceptance

To calculate the expected number of signal $N_{WH\to l\nu b\bar{b}}$, the following equation is used:

$$N_{WH\to l\nu b\bar{b}} = \epsilon_{WH\to l\nu b\bar{b}} \cdot \mathcal{L} \cdot \sigma(p\bar{p} \to WH) \cdot Br(H \to b\bar{b}), \tag{4}$$

where, $\epsilon_{H\to l\nu b\bar{b}}$ is the detection efficiency for signal, $\mathcal{L}$ is the integrated luminosity, $\sigma(p\bar{p} \to WH)$ is WH production cross section in proton antiproton collisions and $BR(H \to b\bar{b})$ is branching ratio for Higgs decaying to $b\bar{b}$. The detection efficiency for signal events is defined as:

$$\epsilon_{WH\to l\nu b\bar{b}} = \epsilon_{Z0} \cdot \epsilon_{trig} \cdot \epsilon_{leptonid} \cdot \epsilon^{MC}_{WH\to l\nu b\bar{b}} \cdot \left(\sum_{l=e,\mu,\tau} BR(W \to l\nu) \right), \tag{5}$$

where $\epsilon^{MC}_{WH\to l\nu b\bar{b}}$ is the fraction of signal events (with $|z_0| < 60$cm) which pass the kinematic and b-tagging requirements. We correct the number of tagged events in the Monte Carlo by multiplying by the b-tagging scale factor. The quantity ϵ_{Z0} is the efficiency for the $|z_0| < 60$ cm cut. The trigger efficiency for the $\not\!\!E_T$ plus jets trigger, ϵ_{trig}, is measured in the data and parameterized as a function of vertex $\not\!\!E_T$. We weight each event in the acceptance according to the derived trigger turn-on curve in Figure 4. We apply a lepton reconstruction scale factor to match the efficiency for isotrk reconstruction to what we measure in $Z \to \mu^+\mu^-$ data (more discucssion in section 5.1. Finally, $Br(W \to l\nu)$ is the branching ratio for leptonic W decay. Each of these factors and their systematic errors are treated separately for each data period and the results are combined weighted by the luminosity of each data period. For the later data periods, where numbers may not have been finalized, preliminary results have been taken from the slides of talks given in the Joint Physics meeting [22].

Samples of PYTHIA $WH \to l\nu b\bar{b}$ Monte Carlo with Higgs boson masses of m_H = 110, 115, 120, 130, 140 and 150 GeV/c^2 are used to estimate $\epsilon^{MC}_{WH\to l\nu b\bar{b}}$. The MC samples were generated using a run range up to period 8.

Table 7 shows the WH production cross section times branching ratio to $b\bar{b}$. The cross sections in Table 7 are combined with the integrated luminosity of 2.101 fb^{-1}and the overall event detection efficiencies to produce the number of expected WH isolated track events shown in Table 8 .

5.1 Isotrk Reconstruction Scale factor

The scale factors are derived analogous to the CMUP scale factors [21] using $Z \to \mu\mu$ events. We select events with one tight CMUP or CMX muon as a tag leg and a high p_T track as a probe leg. We apply the following cuts:

- $81 < m_{ll} < 101$
- $|\Delta z_{ll}| < 4$

M(H)	$\sigma \times BR(H \to b\bar{b})$
110	0.169 pb
115	0.136 pb
120	0.104 pb
130	0.063 pb
140	0.030 pb
150	0.012 pb

Table 7: Theoretical cross section (σ) times branching ratio to $b\bar{b}$ for a variety of higgs masses.

M(H)	N_{Expect} 1 Tag	N_{Expect} 2 Tags
110	1.147	0.398
115	0.941	0.356
120	0.792	0.293
130	0.550	0.184
140	0.281	0.098
150	0.128	0.044

Table 8: Number of expected WH isotrk events in 2.1 fb^{-1}of $\not\!\!E_T$ plus jet triggered data.

- opposite charge
- the tag leg fired the muon trigger (data only)
- the event passed the cosmic veto
- the probe leg satisfies $p_T > 20$
- the probe leg has a muon stub attached

For the events that pass these cuts we calculate the efficiency for passing the track and jet isolation cuts. The ratio of these efficiencies for data and Z Monte Carlo is defined to be the IsoTrack scale factor. Figures 10 to 12 show the isotrk scale factor as function of ϕ, η, and p_T .

5.2 Trigger Systematics: Using CMUP-triggered data to measure the MET+2jet trigger turnon curve

We estimated the systematic uncertainty associated with the $\not\!\!E_T$ trigger turn on by studying the impact of different trigger parameterizations on the signal acceptance. We obtained reasonable alternate trigger parameterizations through the following proceedure:

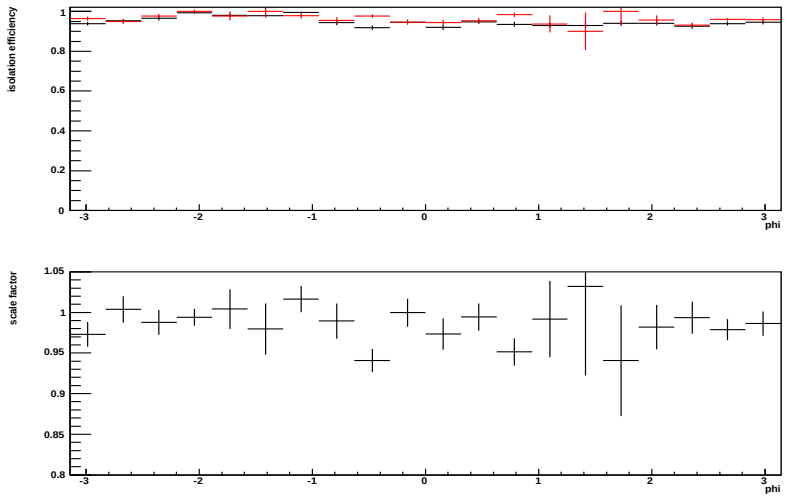

Figure 10: Isolated track reconstruction scale factor vs. lepton ϕ

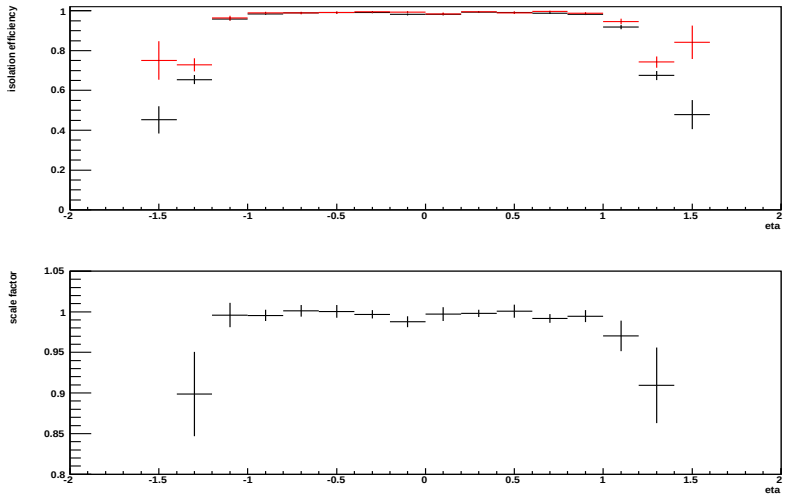

Figure 11: Isolated track reconstruction scale factor vs. η

- We selected CMUP triggered events passing the baseline $\not\!\!E_T$ plus jet trigger requirements (2 jets $E_T > 25$, one central jet, $\Delta R > 1.0$). These events were the trigger efficiency denominator. We parameterized the efficiency for these events to pass the $\not\!\!E_T$ plus jets trigger as a function of vertex met. This provided our nominal or "central" trigger turn-on parameterization.

- We broke the efficiency denominator into 50 subsamples by cutting on jet E_T , η, and ϕ. The sub-samples are selected based on ΔR ¿1.0, jet1 E_T ¿25 GeV, and jet2 E_T in

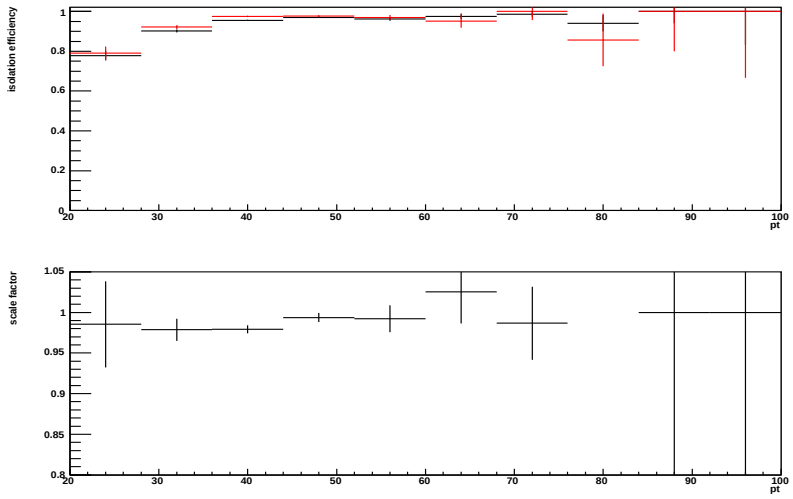

Figure 12: Isolated track reconstruction scale factor vs. p_T

certain range above 25GeV. The ranges are chosen by a script such that each of these subsamples have at least 200 events with MET¿ 30 GeV and MET¡40 GeV (the turnon region). A set of a minum number of events in the turnon region is required for each subsample in order to improve the fit parameters for each turnon curve. Figure 13 shows the norminal turn-on curve and 50 overlaid systematic curves.

- We calculated the signal acceptance for one- and two-tag events separately for each each of the 50 turn-on curves. Figures 14-15 show the signal acceptance for the nominal turn-on and each of the 50 variations.

- We use the $\sigma/mean$ of the acceptance distribution in Figures 14-15, which we meaure to be 2%, as our trigger systematic.

We also studied the impact of the statistical fluctuation of fit parameters on the acceptance. We shifted each of the fit parameters by $\pm 1\sigma$ from their central values and recalculated the acceptance. We found that the statistical uncertainty of each fit was small (0.3%) compared to the overall systematic uncertainty.

We treat the trigger systematic as an uncertainty on the signal normalization.

5.3 Other Systematic Uncertainties on Acceptance

The systematic uncertainties on the acceptance include uncertainties on the jet energy scale, initial and final state radiation, and the b-tagging scale factor. For each source of systematics, we use the same uncertainties as measured by the lepton triggered analysis, using the values for secvtx tag + NN tag for our events with one secvtx tag (there is a 90% overlap of events with one secvtx tag and events with secvtx+NN tag).

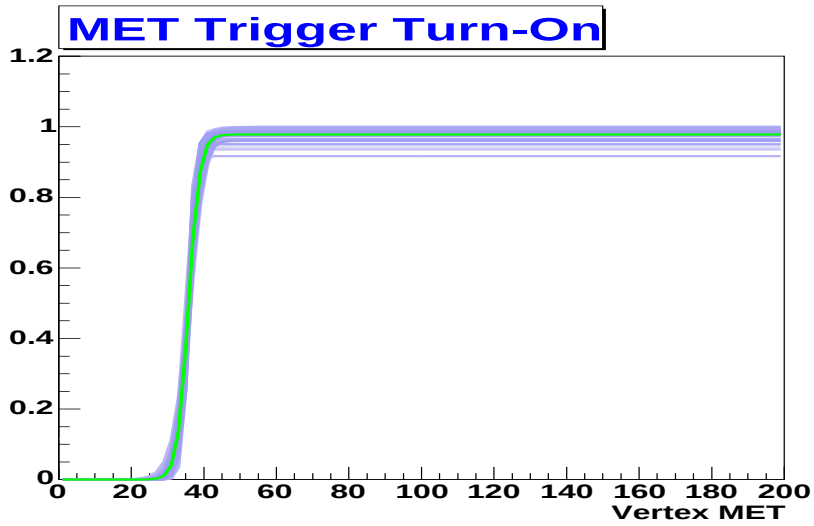

Figure 13: the norminal turn-on curve and 50 overlaid systematic curves, plotted vs vtx met.

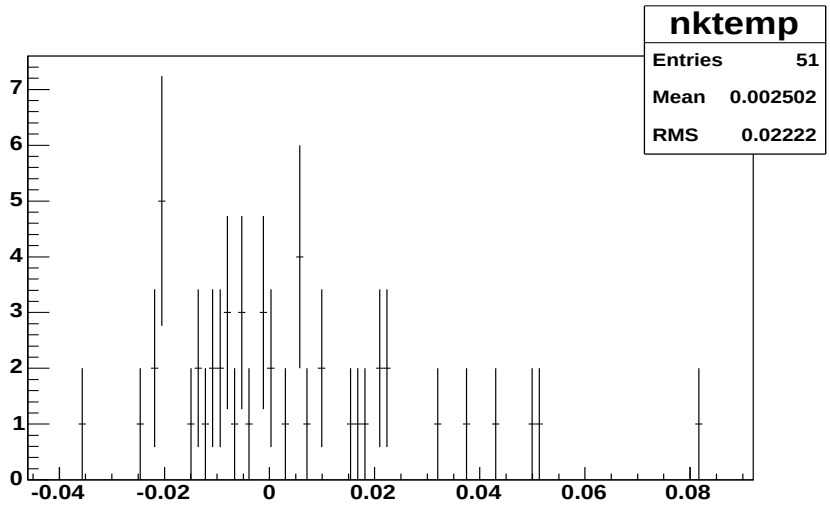

Figure 14: Isolated track 1 tag WH MC event acceptance, shown as a fractional difference from the central, for the 50 variations of $\not\!\!E_T$ plus jet trigger turn-on curves and the nominal trigger turn-on.

1. To obtain the systematic uncertainty from jet energy scale, we use the Higgs sample for a mass of 120 GeV. The jet energies in the WH MC samples are shifted by $\pm 1\sigma$ and the difference from the nominal acceptance is taken as the systematic uncertainty.

2. ISR and FSR systematic uncertainty are estimated by changing the parameters related to ISR and FSR from default values to half and double. Half of difference between the

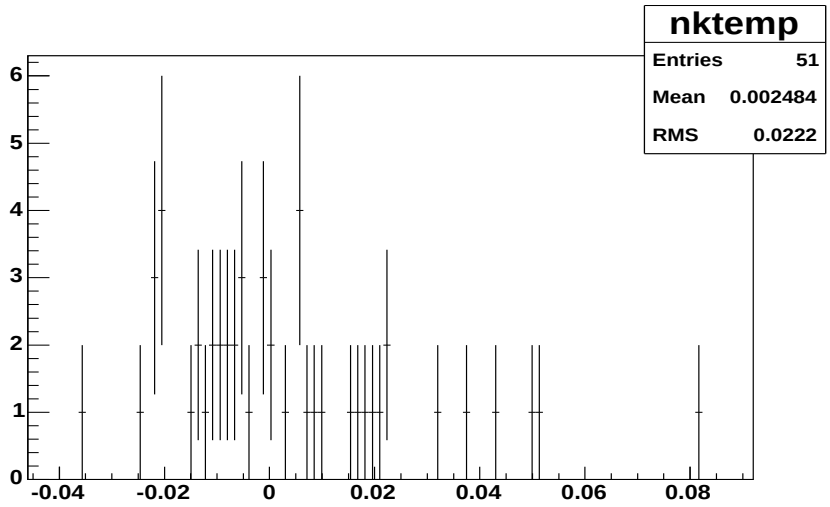

Figure 15: Isolated track 1 tag WH MC event acceptance, shown as a fractional difference from the central, for the 50 variations of $\not\!\!E_T$ plus jet trigger turn-on curves and the nominal trigger turn-on.

two samples is taken as the systematic uncertainly.

3. PDFs uncertainties are evaluated using the standard re-weighting method recommended by Joint Physics [22].

4. The b-tagging scale factor uncertainty comes from the High p_T b-tagging group. We propagate $\pm 1\sigma$ variation of the scale factor through our acceptance calculation and use the relative variation in acceptance as our uncertainty.

5. Luminosity uncertainties are also included in calculating Higgs signal events. This uncertainty assign 6%.

6. **Z+jet Scale Factor Uncertainties:** CDF note 8696 found a change of 4% for the isotrk scale factor mesaured in the Z+2jet sample compared to the Z+0jet sample. To be conservative, we increase our uncertainty on the scale factor from 1% to 6% to accomadate a change in the scale factor that is 1.5 times greater than that observed for the lepton + track search.

7. **Electron/Tau Scale Factor Uncertainties:** Both electrons and single-prong tau decays can be reconstructed as isotrks. Both lepton types make up approximately 15% of the signal composition. To account for this potential difference in the scale factor, we give assign an uncertainty of 25% to the ele+tau piece of the acceptance. This uncertainty would accomodate a variation of the scale factor that is greater than the difference between scale factors used for other lepton types. The extra 25% uncertainty

b-tagging category	Isotrk Reco	Trigger	ISR/FSR	JES	PDF	b-tagging	Total
One tag	8.85%	2%	2.9%	2.3%	1.2%	3.5%	10.06%
ST + ST	8.85%	2%	5.2%	2.5%	2.1%	8.4%	13.8%

Table 9: Systematic uncertainties for each tagging category

on the 15% of isotrk acceptance increases our total isotrk scale factor uncertainty from 6% to 8.85%.

Total systematic uncertainties are listed in Table.9 for each b-tagging category.

6 Neural Network Discriminant

To further improve signal to background discrimination after event selection, we employ an artificial Neural Network (NN) trained on a variety of kinematic variables to distinguish WH from backgrounds. For comparison, we calculate the output of the neural network trained on trigger-lepton events for isolated track events. Figure **??** shows a comparison of this neural network output calculated for CMUP triggered events compared to isolated track events. Because the output is so similar, we conclude that it is sufficient to use the same input variables and neural network training for the isolated track analysis as was used for the triggered lepton analysis. Details of the neural network optimization and training are given in the documentation for the triggered lepton analysis [1]. Recall that this network, which is optimized separately for each Higgs mass, has six input variables (listed below), eleven hidden nodes in a single hidden layer, and one output node. The input variables are listed below:

M_{jj+}**:** This variable is the invariant mass calculated from the two tight jets using Level-5 jet corrections. Furthermore, if there are additional loose jets present ($E_{T,L5} < 12$ GeV and $|\eta| < 2.4$), the loose jet that is closest to one of the two tight jets is included in this invariant mass calculation, if the separation between that loose jet and one of the tight jets is $\Delta R < 0.9$.

$\sum E_T$**(Loose Jets):** This variable is the scalar sum of the loose jet transverse energy (with Level-5 corrections).

p_T **Imbalance:** This variable expresses the difference between the scalar sum of the transverse momenta of all measured objects and the $\not\!\!E_T$. Specifically, it is calculated as $P_T(jet_1) + P_T(jet_2) + P_T(lep) - \not\!\!E_T$.

$M_{l\nu j}^{min}$**:** This is the invariant mass of the lepton, $\not\!\!E_T$, and one of the two jets, where the jet is chosen to give the minimum invariant mass. For this quantity, the p_z of the neutrino is ignored.

ΔR**(lepton-**ν_{max}**):** This is the ΔR separation between the lepton and the neutrino, where the p_z of the neutrino is taken from by choosing the solutions from the quadratic equations for the W mass constraint with the largest $|p_z|$.

$P_T(W + H)$**:** This is the total transverse momentum of the W plus two jets system, $P_T(\vec{lep} + \vec{\nu} + \vec{jet}_1 + \vec{jet}_2)$.

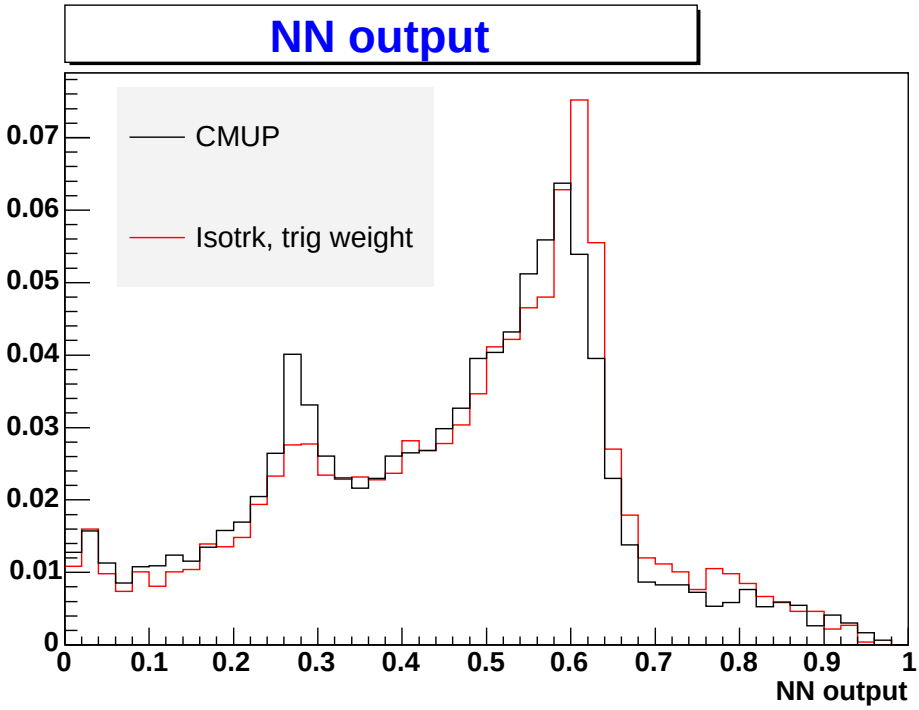

Figure 16: Comparison of NN output for signal ($M_H = 120$ GeV) events passing CMUP selection (black) and Isotrk selection (red). The plots are drawn with equal areas.

7 Kinematic Shape

We check the kinematics each tagging category to see that the background composistions and modeling are well understood.

7.1 Pretag

Figures 17 through 21 show the kinematics of pretag sample.

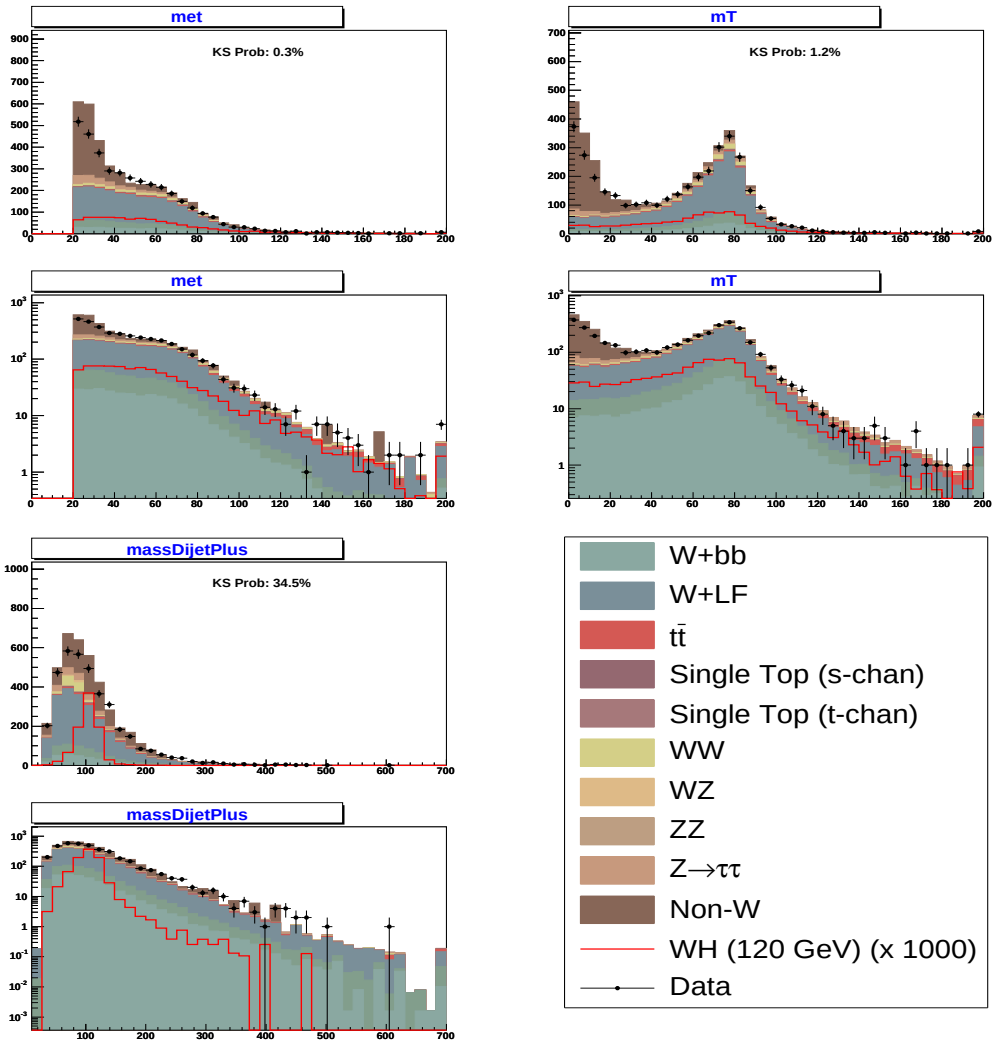

Figure 17: Comparison of expected background, observed data, and WH signal kinematics in the pretag sample.

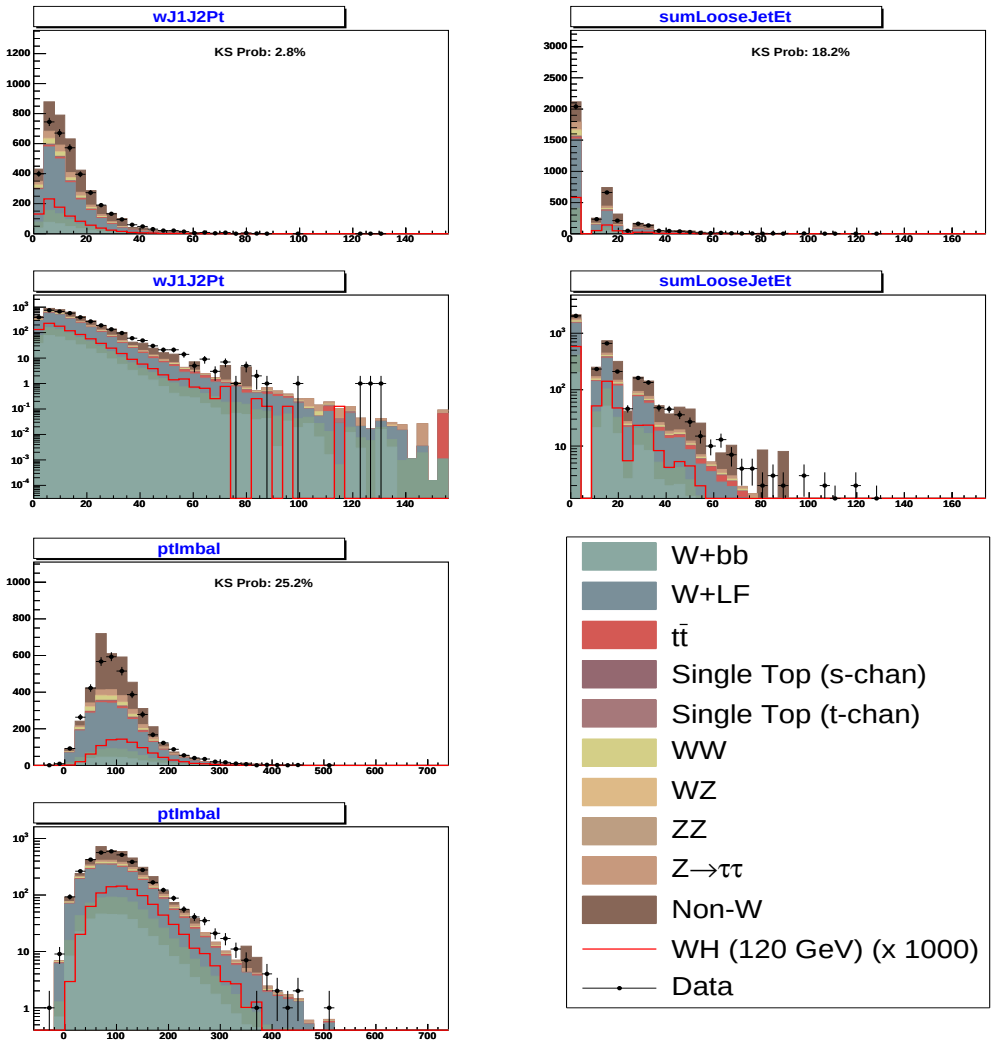

Figure 18: Comparison of expected background, observed data, and WH signal kinematics in the pretag sample.

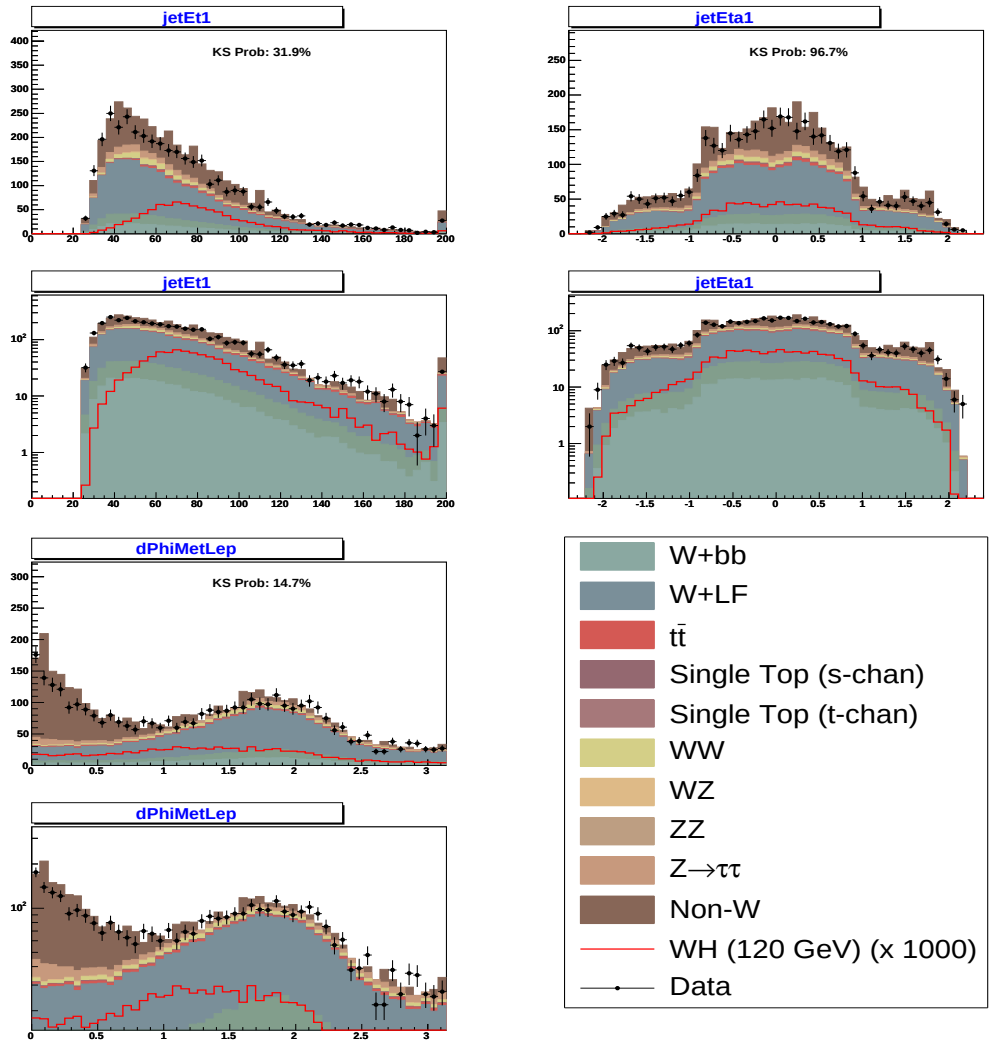

Figure 19: Comparison of expected background, observed data, and WH signal kinematics in the pretag sample.

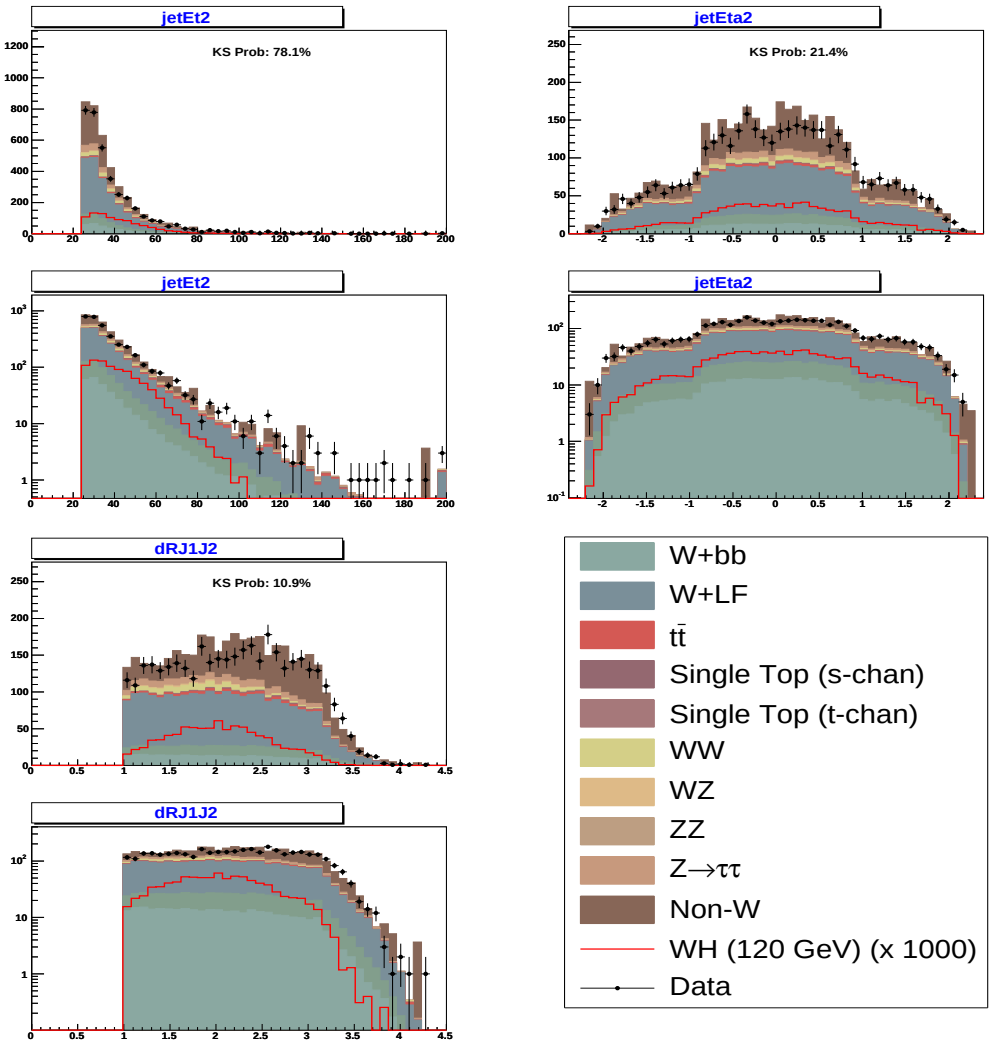

Figure 20: Comparison of expected background, observed data, and WH signal kinematics in the pretag sample.

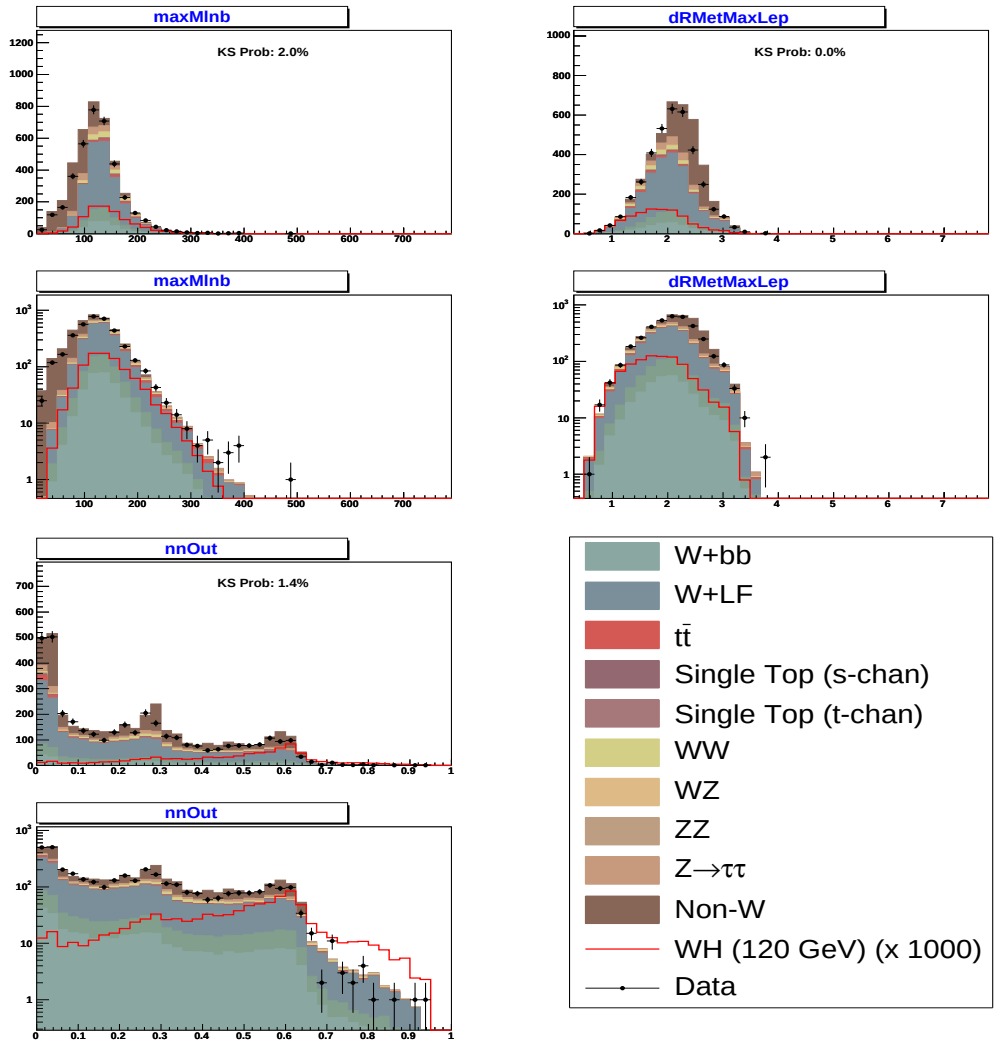

Figure 21: Comparison of expected background, observed data, and WH signal kinematics in the pretag sample.

7.2 One Secvtx Tag

Figures 22 through 26 show the kinematics of one tag sample.

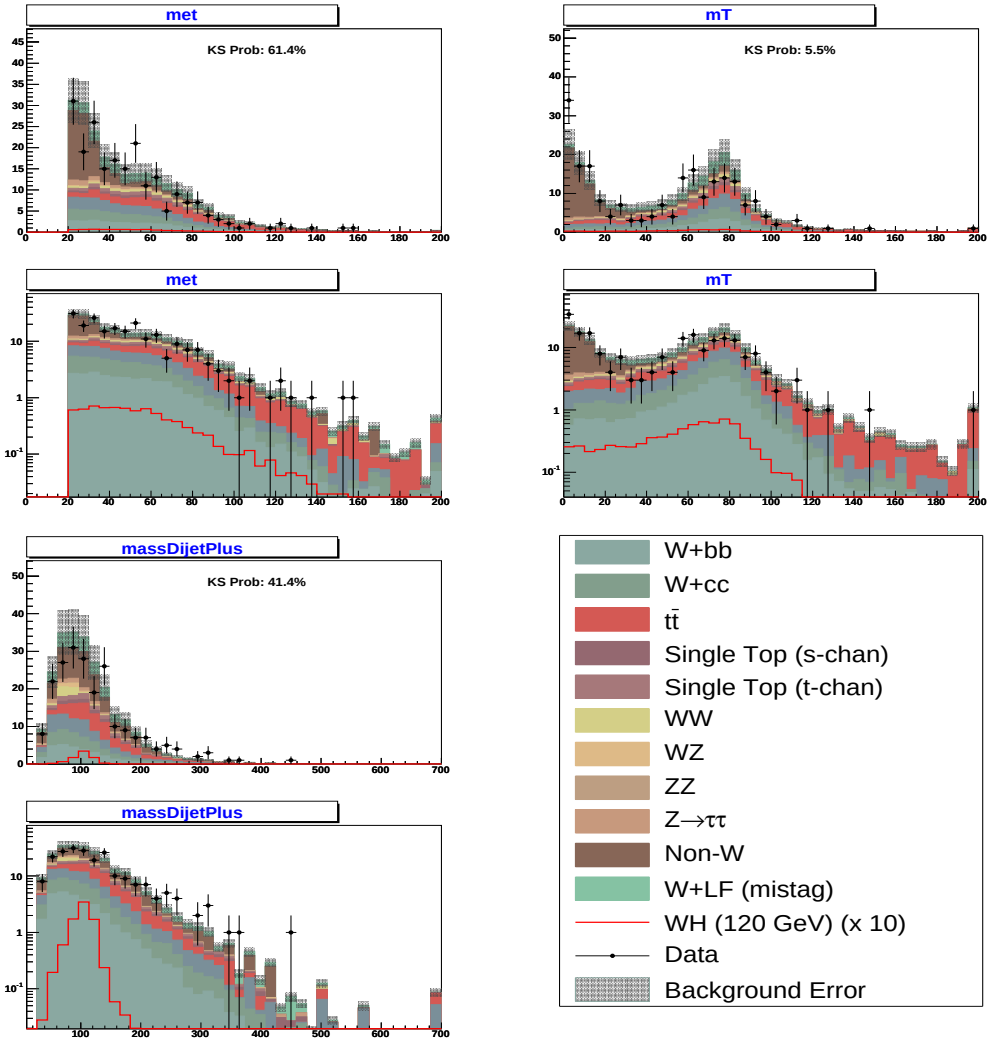

Figure 22: Comparison of expected background, observed data, and WH signal kinematics in the one secvtx tag sample.

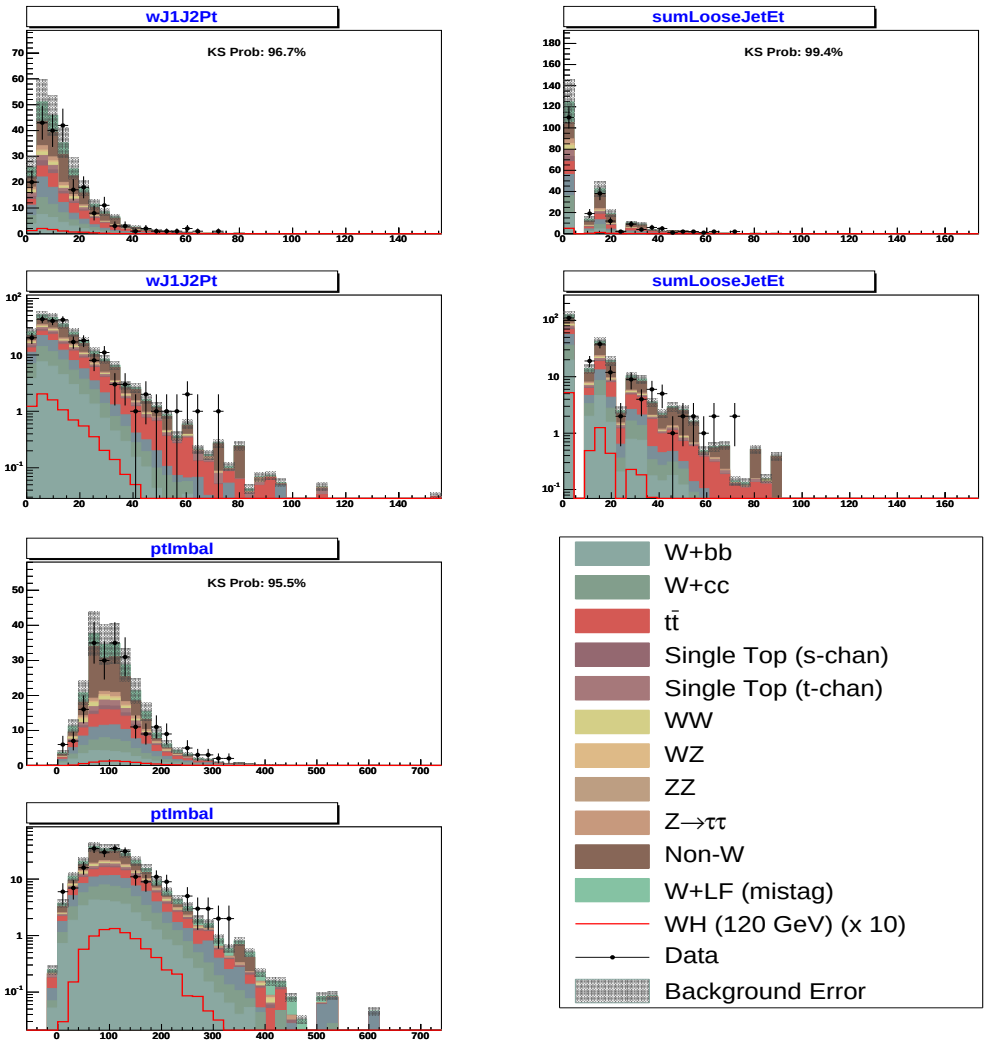

Figure 23: Comparison of expected background, observed data, and WH signal kinematics in the one secvtx tag sample.

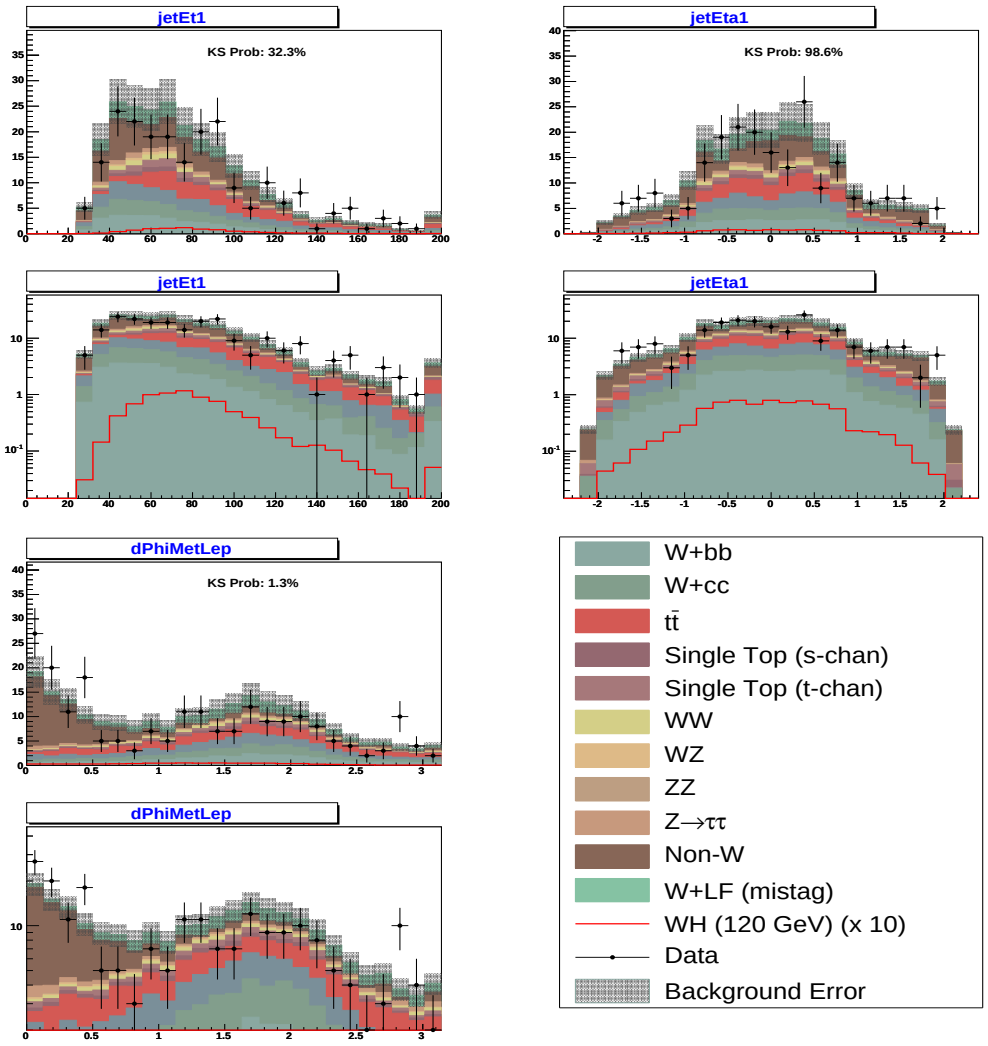

Figure 24: Comparison of expected background, observed data, and WH signal kinematics in the eq1tag sample.

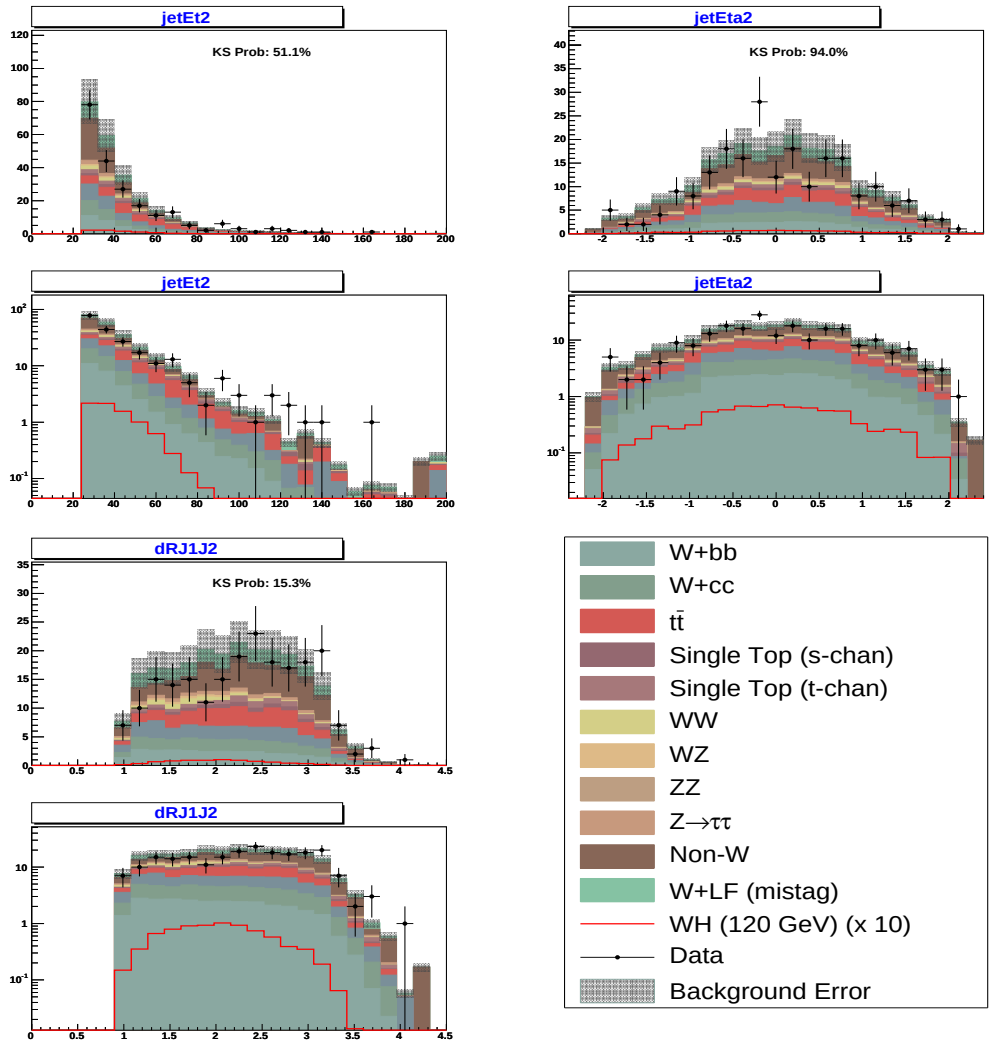

Figure 25: Comparison of expected background, observed data, and WH signal kinematics in the eq1tag sample.

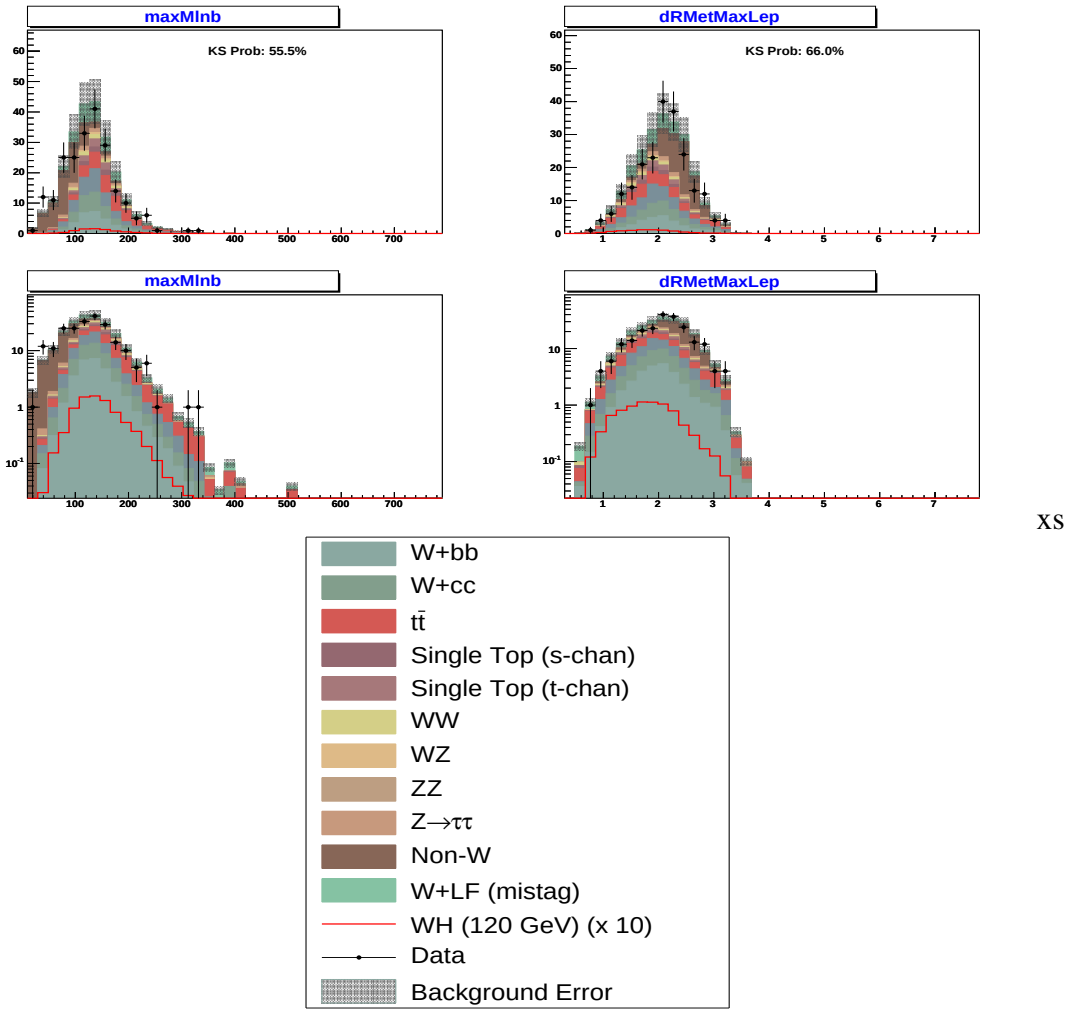

Figure 26: Comparison of expected background, observed data, and WH signal kinematics in the one secvtx tag sample.

7.3 Double Secvtx Tag

Figures 27 through 31 show the kinematics of double tag sample.

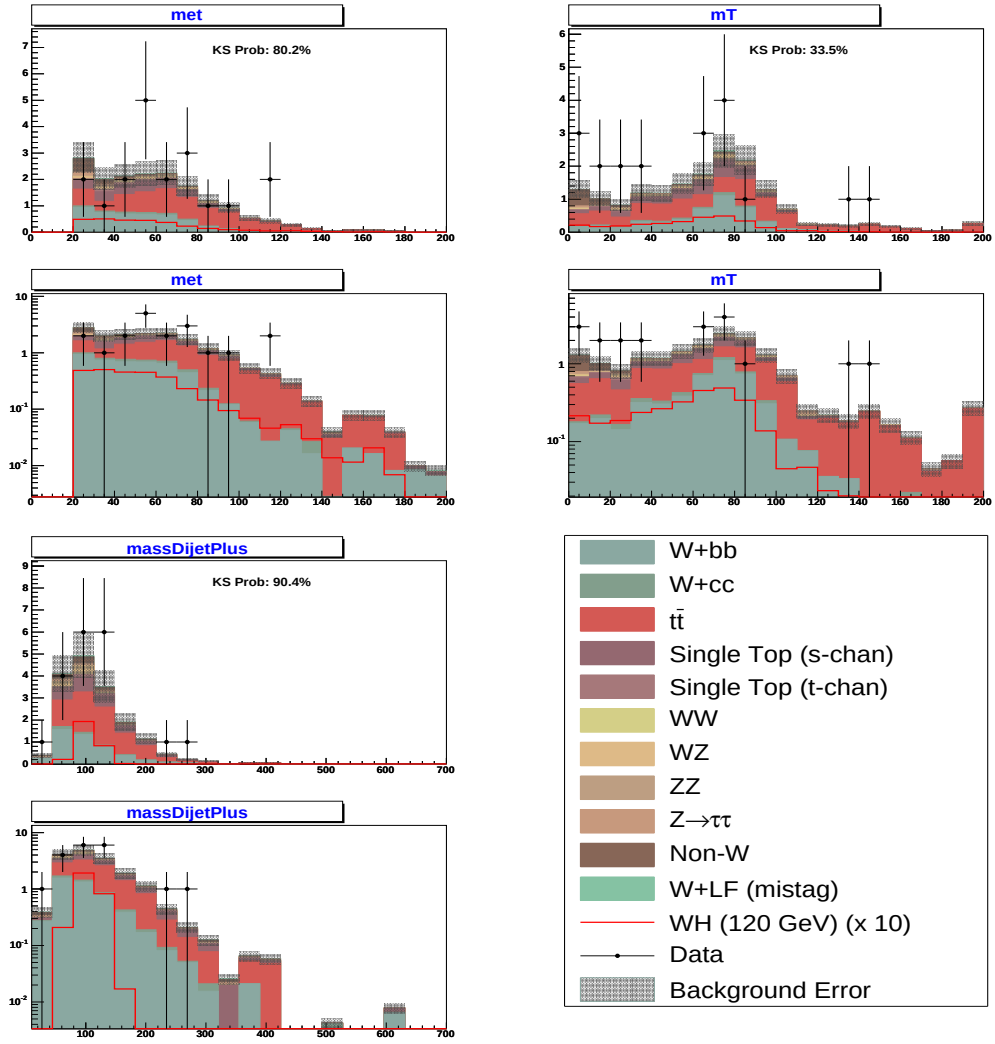

Figure 27: Comparison of expected background, observed data, and WH signal kinematics in the two secvtx tag sample.

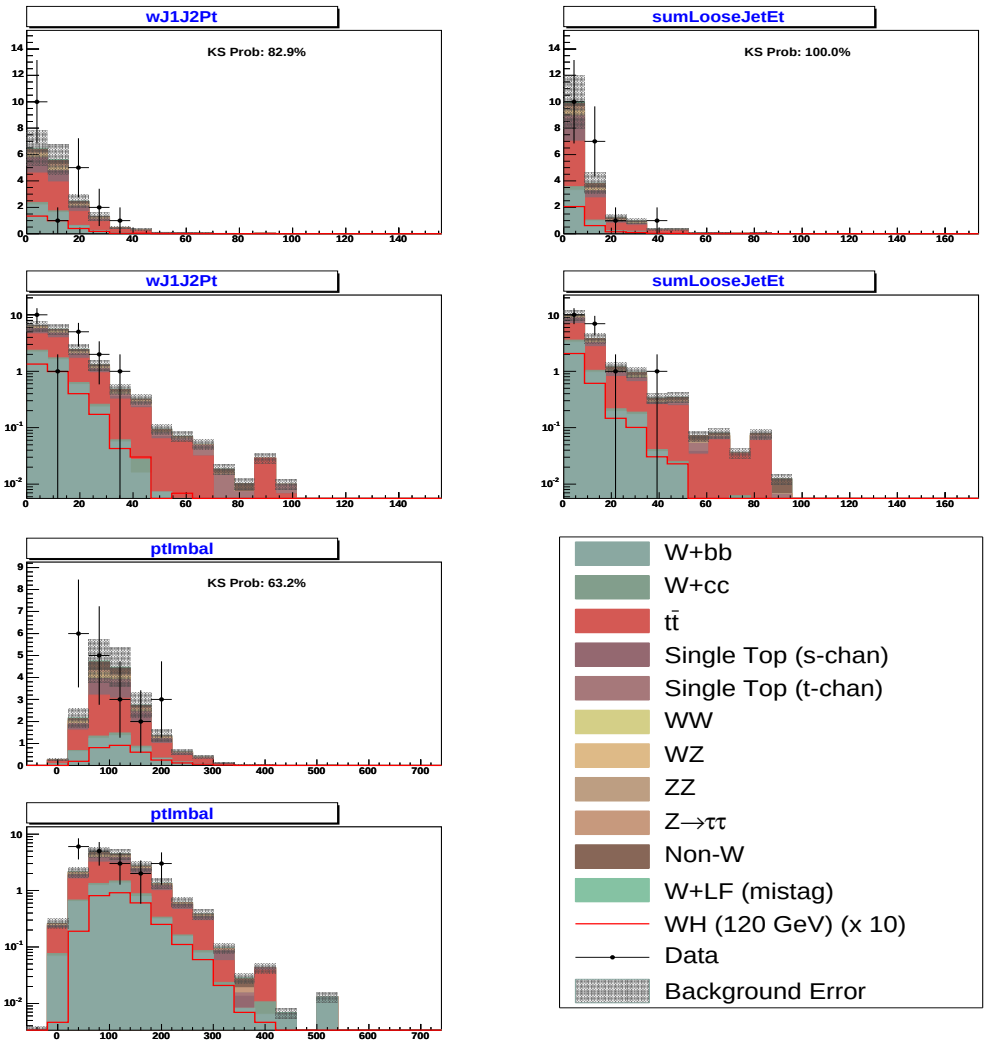

Figure 28: Comparison of expected background, observed data, and WH signal kinematics in the two secvtx tag sample.

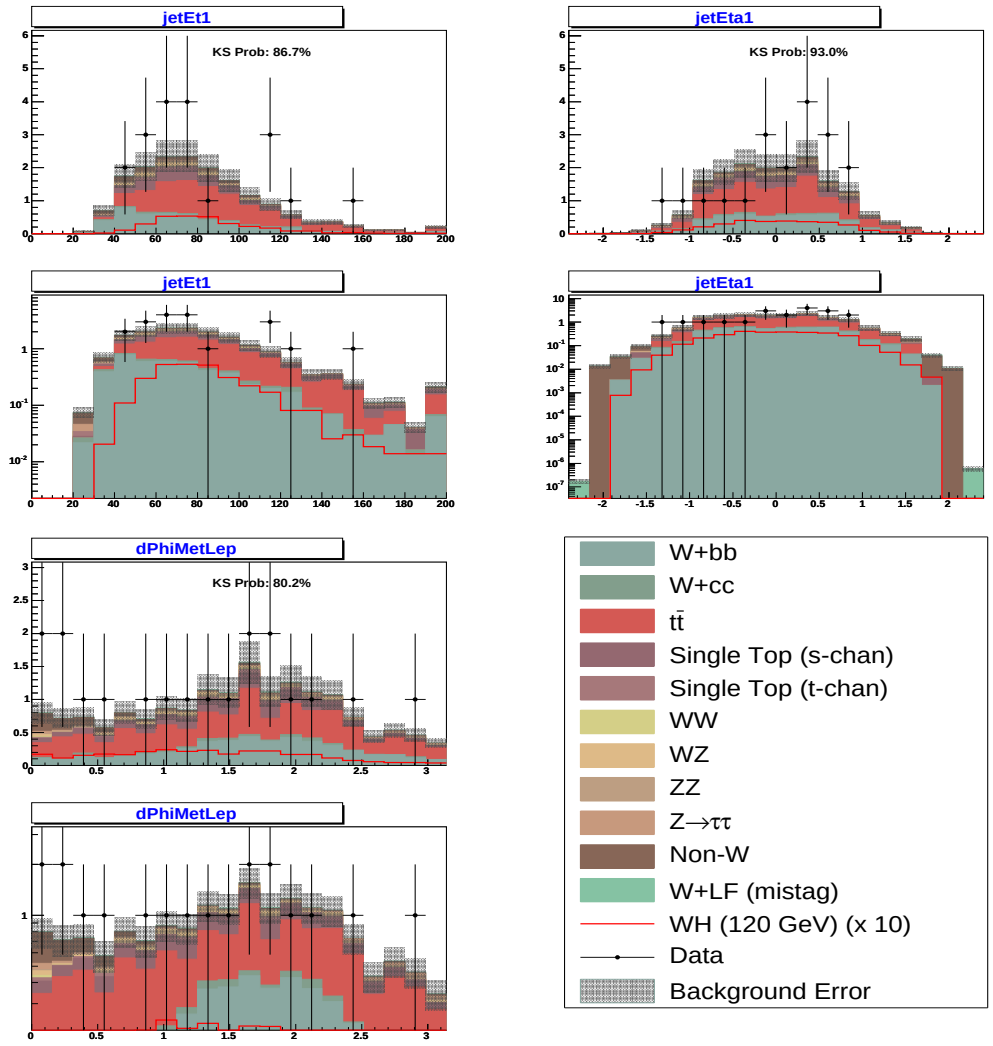

Figure 29: Comparison of expected background, observed data, and WH signal kinematics in the pretag sample.

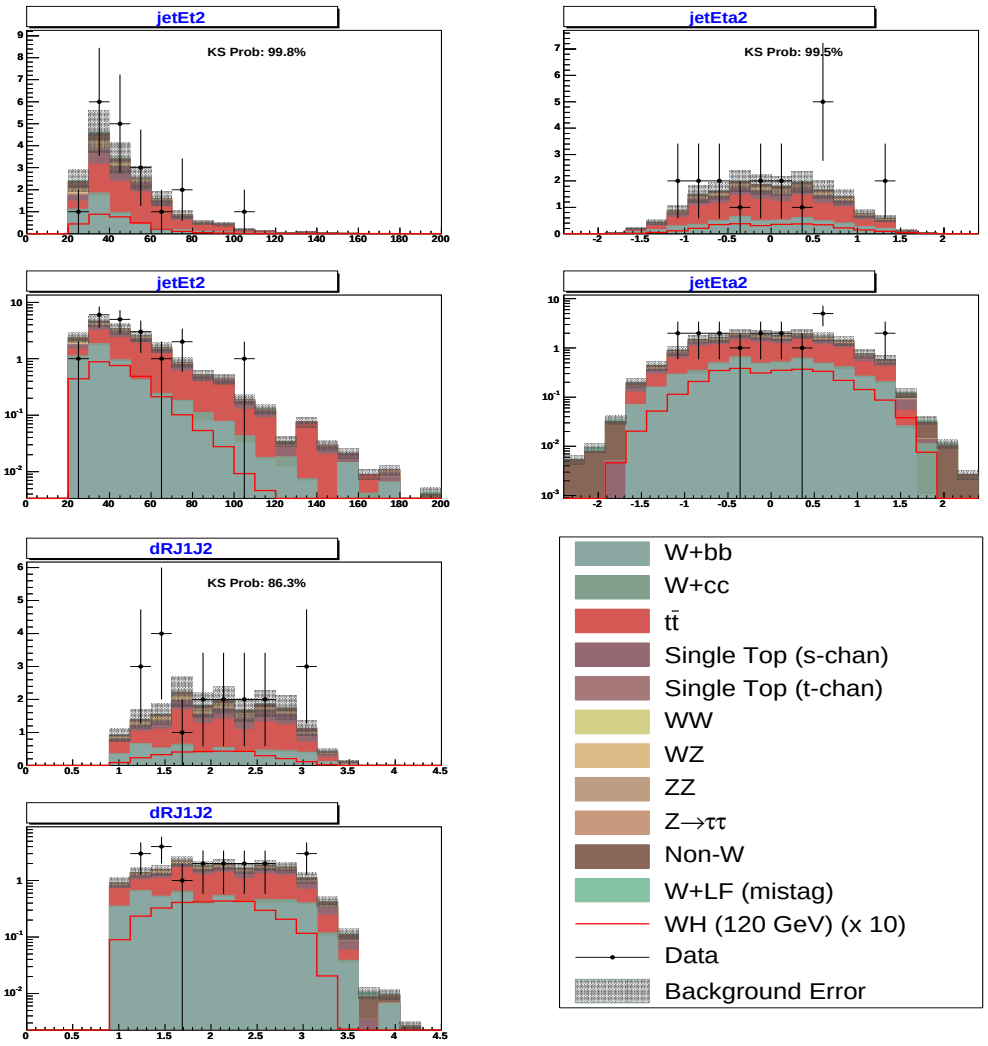

Figure 30: Comparison of expected background, observed data, and WH signal kinematics in the pretag sample.

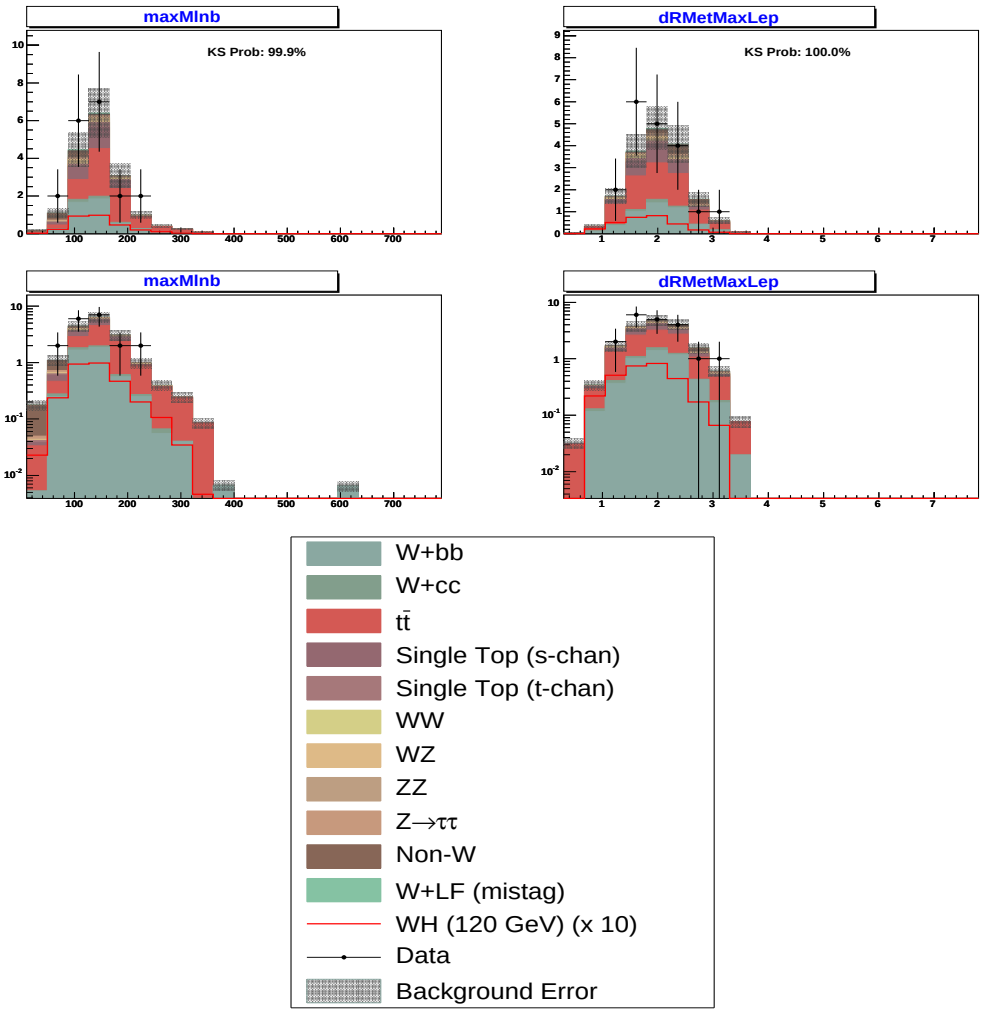

Figure 31: Comparison of expected background, observed data, and WH signal kinematics in the two secvtx tag sample.

8 Sensitivity and Results

We search for evidence for an excess of WH signal events over the background prediction in the Neural Network output distributions for the two tagging categories. Figure 32 shows the NN output distributions for the search regions. We find no evidence for and excess of signal, so set a 95% confidence level upper limit on the production cross section times branching ratio. We check out limits in the individual tag channels, then perform a simultaneous search across both channels for optimal sensitivity.

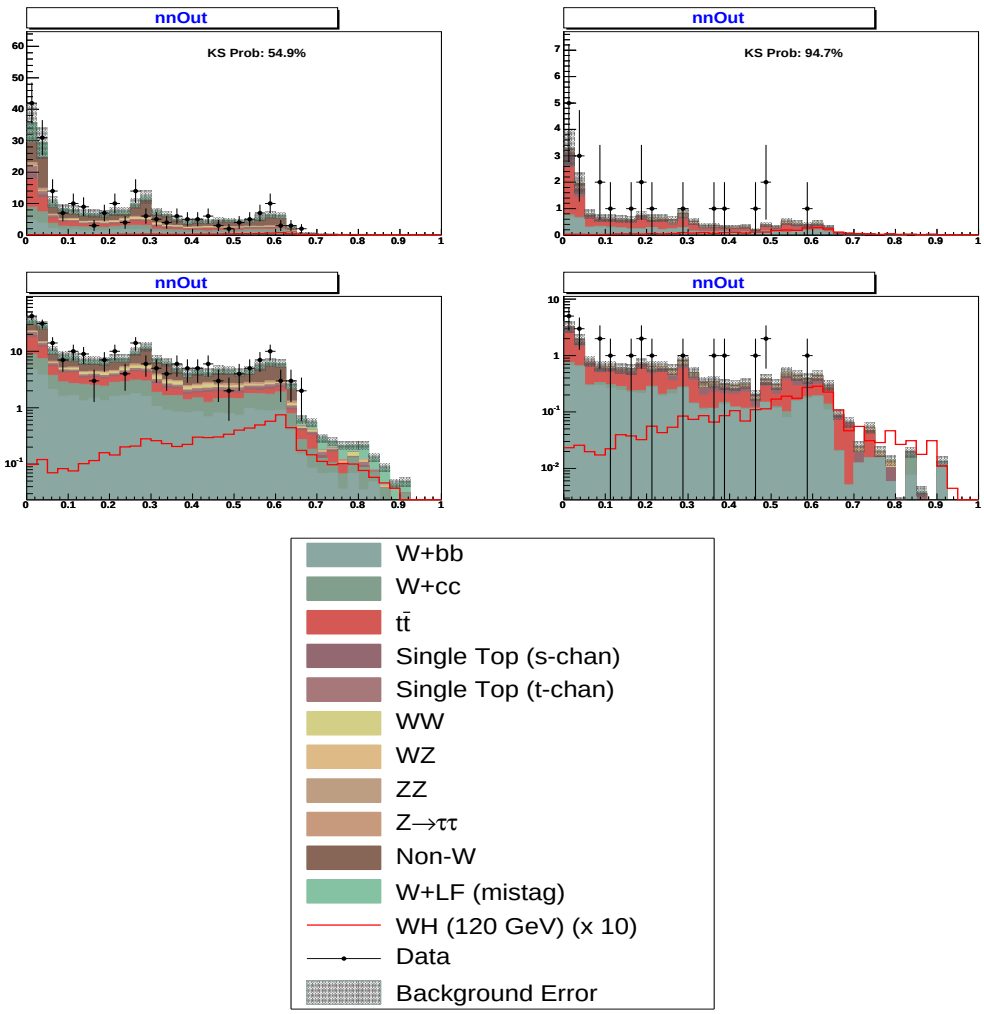

Figure 32: Comparison of NN output for signal ($M_H = 120$ GeV), expected backgrounds, and observed data.

We use `mclimit` [9] to extract the 95% confidence limit on WH production. The `mclimit` tool throws pseudo experiments that incorporate both Poisson and systematic

M(H)	Observed Limit	Expected Limit
110	18.176	21.1732
115	22.0979	26.4423
120	22.7031	29.7255
130	33.7763	41.4503
140	69.6986	75.4635
150	154.668	150.489

Table 10: Expected and observed limits as a function of Higgs mass for the one tag channel.

M(H)	Observed Limit	Expected Limit
110	18.3792	19.3694
115	20.1663	21.9661
120	23.6865	26.2869
130	38.4107	41.3261
140	88.8366	76.9336
150	189.303	164.031

Table 11: Expected and observed limits as a fucntion of higgs mass for the two tag channel (ST+ST).

fluctuations of the signal and background templates. The limit setting proceedure used by `mclimit` has been cross-checked against the binned likelihood technique used in the lepton-triggered analysis. The two techniques have been demonstrated to give equivalent results.

Tables 10 through 12 detail the expected and observed limits at the various Higgs mass points. Figures 33 through 35 display the information in the tables.

Figure 36 shows the expected and observed limits for the central leptons, phoenix electrons, isolated tracks, and the combined search over all lepton types. The limits from the combined search are summarized in Table 13. Including isolated tracks with the central and phoenix analysis increases the sensitivity by 17% for M_H = 115 GeV/c^2, which consists of 25% improvement of acceptance and 10% of more luminosity.

9 Conclusions

We have presented the results of a search for the Standard Model Higgs boson via associated WH production and decay to $b\bar{b}$. We find that for the dataset corresponding to integrated luminosity of 2.1fb^{-1}, the observed data for each tagged events agrees with the SM background predictions within the systematic uncertainties. Therefore we set upper limit on the Higgs production cross section using the single and double tagged channels. The observed limit using the neural network output distribution is $\sigma(p\bar{p} \rightarrow W^{\pm}H) \times BR(H \rightarrow b\bar{b})$ ranging from 11.3 $\times$ SM (for m_h = 110 GeV/c^2) to 126.1 $\times$ SM (for m_h = 150 GeV/c^2) at 95%

M(H)	Observed Limit	Expected Limit
110	11.0946	13.5673
115	12.4743	15.7373
120	13.409	18.5404
130	20.7579	27.489
140	52.283	49.3025
150	114.457	104.246

Table 12: Expected and observed limits as a function of Higgs mass for the combined search of single and double tag events.

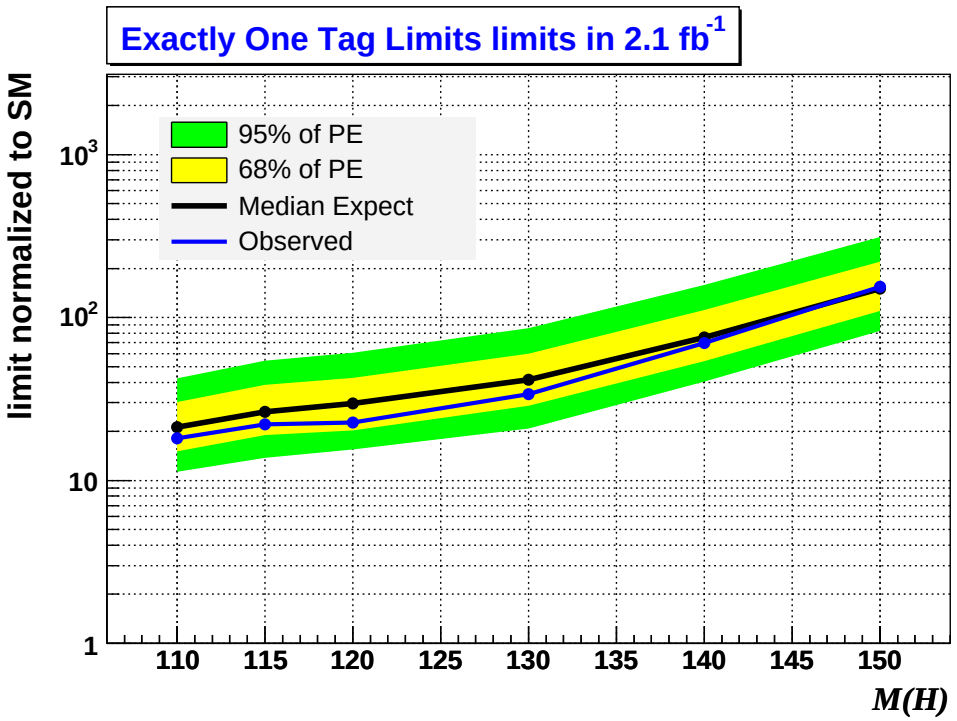

Figure 33: Expected and observed limits for events with one secvtx tag.

confidence level.

References

[1] T. Masubuchi et al., "Search for Higgs Boson Production in Association with W Boson with 1.7fb-1", CDF Note 9136 2, 23

[2] See `http://www-cdf.fnal.gov/internal/physics/top/RunIITopProp/gen6Sum06/lumi_v19.html` 4

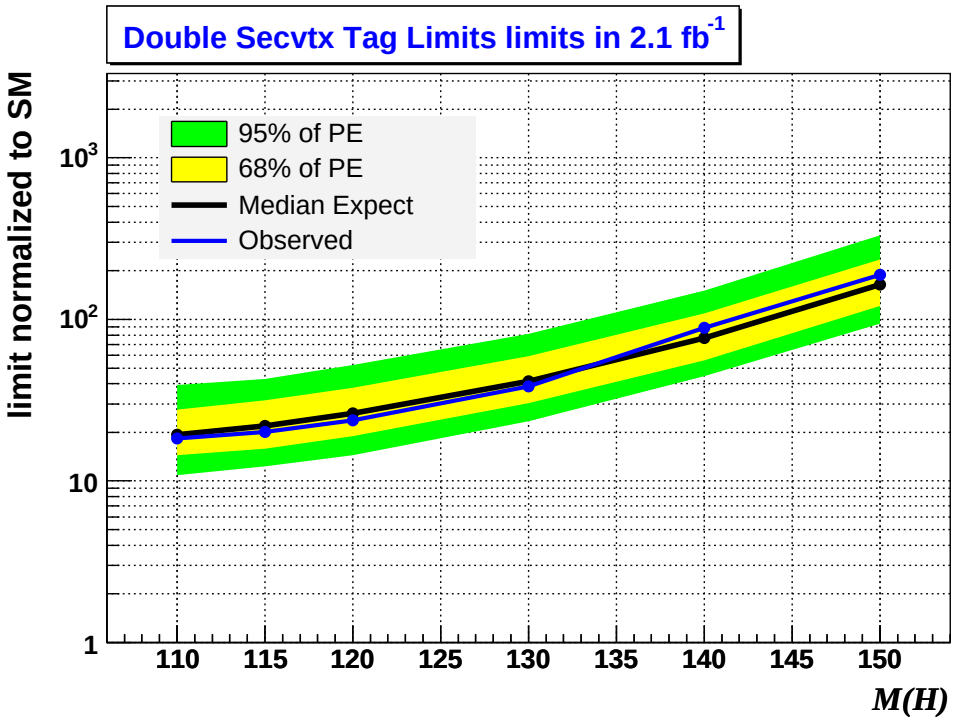

Figure 34: Expected and observed limits for events with two secvtx tags

M(H)	Observed Limit	Expected Limit
110	5.26	5.52
115	6.4	6.4
120	6.8	7.6
130	11.5	11.0
140	30.0	20.2
150	68.9	48.1

Table 13: Expected and observed limits for the WH search using all lepton types.

[3] J. Incandela, C. Mills, et al., "A Measurement of the ttbar Dilepton Cross-section in the 1.1 fb-1 Lepton + Isolated Track Sample" CDF Note 8696 4

[4] B. Parks et al, "Low Mass Higgs Serach in Met Plus Jets Data Sample" CDF Note 8678 5

[5] A. Apresyan et al, "Search for the Standard Model Higgs boson in the Missing Et and b-jet Signature" CDF Note 8911 5

[6] B. Casal, C. Group, et al "Increasing Muon Acceptance with the MET Plus Jet Triggers", CDF Note 9105 5, 6

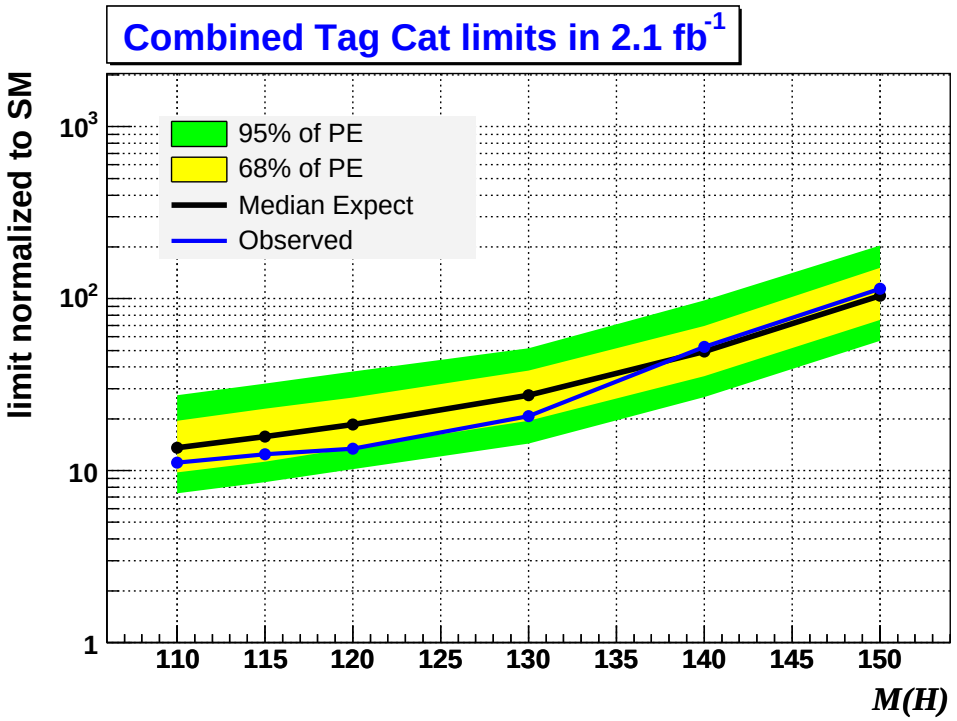

Figure 35: Expected and observed limts for a combined isotrk search in the single and double tag channels.

[7] Franklin, Grinstein, Guimaraes da Costa, Lannon, Schwarz, Sherman and Taffard, "Method 2 Backgrounds for 1.12/fb Lepton+Jets Analysis, CDF Note 8766 7, 9

[8] J. Adelman, T. Schwarz, J. Slaunwhite, et al. "Method II For You", CDF Note 9185 7, 8, 9

[9] T. Junk, "Sensitivity, Exclusion, and Discovery with Small Signals, Large Backgrounds, and Large Systematics" CDF Note 8128 40

[10] H.Bachacou, P.Lujan, M.McFarlane, W.Yao, Advanced Heavy Flavor Tagging Using a Neural Network, CDF Note 7742

[11] Y. Kusakabe et al., "Search for Standard Model Higgs Boson Production in Association with $W^{\pm}$ Boson at CDF with $\int \mathcal{L}dt$ = 695 pb^{-1}, CDF Note 8194

[12] Y. Kusakabe et al., "Search for Standard Model Higgs Boson Production in Association with a $W^{\pm}$ Boson at CDF with $\int \mathcal{L}dt$ = 1.0 fb^{-1}, CDF Note 8355

[13] C. Cully, *et al.* "Calibration of Heavy-Flavor Production in W + 1 Jet Data," CDF Note 9187.

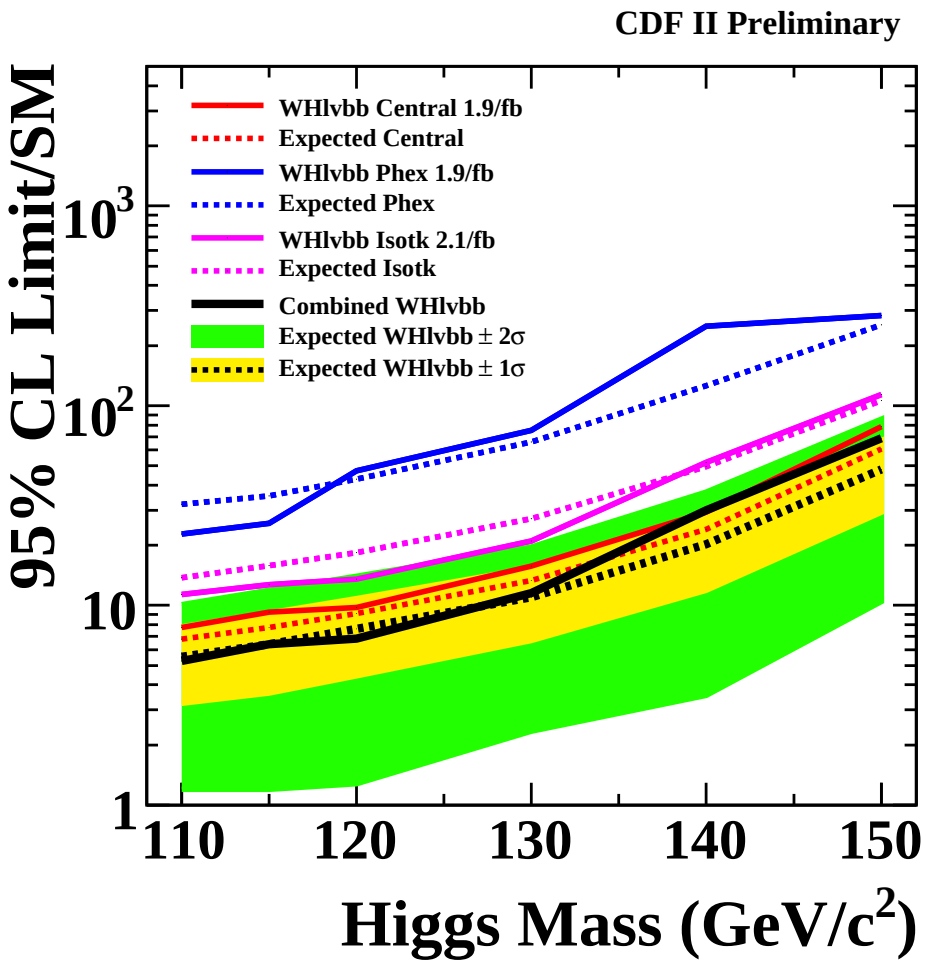

Figure 36: Expected and observed limits for the search using all lepton types. Adding isotrks improves the limit at M_H = 115 GeV/c^2 by 17%

[14] S. Grinstein, D. Sherman, "SecVtx Scale Factors and Mistag Matrices for the 2007 Summer Conferences", CDF Note 8910

[15] Grintein, Guimaraes da Costa, Shrman, "SecVtx Mistag Asymmetry for Winter 2007", CDF Note 8626

[16] Ford Garberson, Enrique Palencia, "Jet Probability B-Tag Efficiency Measurement Using Muon Transverse Momemtum for 1.2 fb^{-1} ", CDF Note 8882

[17] http://www.physics.ucdavis.esu/ conway/research/higgs/higgs.html

[18] http://ncdf70.fnal.gov:8001/PerfIDia/PerfIDia.html

[19] Han, Boisvert, "Trigger Efficiencies for the High Et Central Electron in the Gen6 data", CDF Note 8629

[20] Hare, Halkiadakis, Spreitzer, "Electron ID Efficiency and Scale Factors for Winter 2007 Analyses", CDF Note 8614

[21] Grundler, Lovas, Taffard, "High-Pt muons recommended cuts and efficiencies for Winter 2007", CDF Note 8618

[22] http://www-cdf.fnal.gov/internal/physics/joint_physics/index.html

[23] H. Bachacou, C. Feretti, J. Nielse, W.Yao, "Heavy Flavor contributions to the SECVTX-tagged W+Jets sample" CDF note 7007

[24] J. Efron et al., "Improved search for ZH to llbb in 1 fb-1", CDF Note 8704.

[25] D. Hirschbühl, J. Lück, Th. Müller, A. Papaikonomou, Th. Peiffer, M. Renz, S. Richter, I. Schall, J. Wagner-Kuhr, W. Wagner, "Search for single top-quark production with neural networks using 1.92 fb-1", CDF Note 9107

[26] Bo-Young Han, Eva Halkiadakis, "MET PEM trigger efficiency for Pheonix electrons", CDF Note 7940

[27] D. Hare, E. Halkiadakis, T. Spreitzer, " Electron ID Efficiency and Scale Factors for Winter 2007 Analyses" CDF Note 8614

[28] Michael Feindt, "A Neural Bayesian Estimator for Conditional Probability Densities", physics/0402093

[29] T. Chwalek, M. Feindt, D. Hirschbuehl, T. Müller, M. Renz, S. Richter, W. Wagner, " Documentation of the updated Neural Network b Tagger used for Single-Top Analyses", CDF Note 8903